

# Insights from Modeling Magnetar-driven Light Curves of Stripped-envelope Supernovae

Amit Kumar<sup>a,b,\*</sup>

<sup>a</sup>Department of Physics, Royal Holloway - University of London, Egham Hill, Egham, TW20 0EX, UK

<sup>b</sup>Department of Physics, University of Warwick, Gibbet Hill Road, Coventry, CV4 7AL, UK

## ARTICLE INFO

**Keywords:**  
 Supernovae  
 Gamma-ray bursts  
 Magnetars  
 Light-curve analysis  
 Statistical analysis  
 Semi-analytical modelling.

## ABSTRACT

This work presents the semi-analytical light curve modelling results of 11 stripped-envelope SNe (SESNe), where millisecond magnetars potentially drive their light curves. The light-curve modelling is performed utilizing the  $\chi^2$ -minimisation code MINIM considering millisecond magnetar as a central engine powering source. The magnetar model well regenerates the bolometric light curves of all the SESNe in the sample and constrains numerous physical parameters, including magnetar's initial spin period ( $P_i$ ) and magnetic field ( $B$ ), explosion energy of supernova ( $E_{\text{exp}}$ ), progenitor radius ( $R_p$ ), etc. Within the sample, the superluminous SNe 2010kd and 2020ank exhibit the lowest  $B$  and  $P_i$  values, while the relativistic Ic broad-line SN 2012ap shows the highest values for both parameters. The explosion energy for all SESNe in the sample (except SN 2019cad), exceeding  $\gtrsim 2 \times 10^{51}$  erg, indicates there is a possibility of a jittering jet explosion mechanism driving these events. Additionally, a correlation analysis identifies linear dependencies among parameters derived from light curve analysis, revealing positive correlations between rise and decay times,  $P_i$  and  $B$ ,  $P_i$  and  $R_p$ , and  $E_{\text{exp}}$  and  $R_p$ , as well as strong anti-correlations of  $P_i$  and  $B$  with the peak luminosity. Principal Component Analysis is also applied to key parameters to reduce dimensionality, allowing a clearer visualization of SESNe distribution in a lower-dimensional space. This approach highlights the diversity in SESNe characteristics, underscoring unique physical properties and behaviour across different events in the sample. This study motivates further study on a more extended sample of SESNe to look for millisecond magnetars as their powering source.

## 1. Introduction

Stripped-envelope supernovae (SESNe) originate from the core-collapse of massive stars ( $> 8 M_\odot$ ; Heger et al. 2003; Smartt 2009) that have stripped off their outer H/He-envelopes before the explosion, e.g., massive Wolf-Rayet stars ( $\gtrsim 20 M_\odot$ ; Woosley et al. 1995; Georgy et al. 2009; Yoon 2015) or low-mass stars in binary systems ( $\gtrsim 11 M_\odot$ ; Yoon et al. 2010; Smith et al. 2011; Smith 2014; Solar et al. 2024). Several potential mechanisms exist by which SESNe could stripped off their outer H/He-envelopes, such as steady line-driven winds (Conti, 1975; Puls et al., 2008; Pauldrach et al., 2012; Björklund et al., 2023; Curé and Araya, 2023), eruptive episodes of mass-loss (Smith and Owocki, 2006; Beasor et al., 2020; Bonanos et al., 2024) and/or mass-transfer to a binary companion through Roche Lobe overflow (Nomoto, 1984; Podsiadlowski et al., 2004; Yoon et al., 2010; Lyman et al., 2016; Gilkis et al., 2019; Drout et al., 2023).

SESNe can be distinguished from Type II and Type Ia SNe respectively through the absence of Balmer and Si II features in their early spectra (Filippenko 1997; Gal-Yam 2017; Prentice and Mazzali 2017). Further classification of SESNe leads to subclasses, such as Type Ib and Ic, based on the presence and absence of He-features in their spectra, respectively. Type Ic SNe can further be subdivided into superluminous SNe (SLSNe-I), Ic broad-line (Ic-BL), and gamma-ray bursts (GRBs) associated SNe (GRB-SNe); see Modjaz et al. (2019). SLSNe-I, distinguished by their 10–100 times higher luminosity compared to classical SNe, and W-shaped O II features in the bluer part of their near-peak optical spectra (Quimby et al., 2011; Inserra, 2019; Nicholl, 2021; Gomez et al., 2024; Moriya, 2024). SNe Ic-BL are characterised by broad absorption spectral features, indicating high ejecta expansion velocity ( $V_{\text{exp}} \gtrsim 20,000 \text{ km s}^{-1}$ ; Galama et al. 1998; Modjaz et al. 2016; Taddia et al. 2019). Some Ic-BL SNe are also found to be associated with GRBs and are thus termed GRB-SNe (Woosley and Bloom, 2006; Cano et al., 2017; Kumar et al., 2024; Kumar and

\*Corresponding author

 amitkundu515@gmail.com; amit.kumar@rhul.ac.uk (A. Kumar)  
 ORCID(s): 0000-0002-4870-9436 (A. Kumar)

Sharma, 2024). There also exists a unique case of an SLSN associated with an ultra-long (UL) GRB 111209A, SN 2011kl (Greiner et al., 2015; Kann et al., 2019), opening new avenues for exploring connections between SLSNe-I and GRBs. Additionally, within Type Ic subclasses, there are other peculiar events, such as relativistic Ic-BL SNe with highly relativistic ejecta than those of Ib/c SNe and comparable to sub-energetic GRBs (e.g., SNe 2009bb; Levesque et al. 2010; Pignata et al. 2011, 2012ap; Liu et al. 2015; Milisavljevic et al. 2015 and 2023adta; Siebert et al. 2024), see Margutti et al. (2014).

Type Ic-BL SNe are among the most energetic SNe, with explosion energies ( $E_{\text{exp}}$ ) usually reaching  $\gtrsim 10^{52}$  erg (Maeda et al., 2003; Janka et al., 2016; Prentice et al., 2016; Cano et al., 2017), higher than those of other subtypes of SESNe, those exhibit explosion energies in the range of  $\approx 10^{50-52}$  erg (Utrobin et al., 2015; Taddia et al., 2018; Gal-Yam, 2019; Burrows and Vartanyan, 2021). Studies have shown that the explosion energy of SNe can be helpful in probing their explosion mechanism (Shishkin and Soker 2023, see also Soker 2024 for a recent review). The two popular theoretical mechanisms that explain the explosion of SESNe are the delayed neutrino explosion mechanism (Bethe and Wilson, 1985; Burrows et al., 2020; Bollig et al., 2021; Burrows and Vartanyan, 2021; Bocchieri and Roberti, 2024; Yamada et al., 2024) and the jittering jet explosion mechanism (JJEM; Soker 2010; Papish and Soker 2011; Gilkis and Soker 2015; Antoni and Quataert 2022; Soker 2022b, 2023; Bear and Soker 2025). Whereas, the delayed neutrino explosion mechanism can not explain the SNe with  $E_{\text{exp}} \gtrsim 2 \times 10^{51}$  erg (Fryer et al., 2012; Sukhbold et al., 2016; Gogilashvili et al., 2021). Hence, the exceptionally high explosion energy of most of the Type Ic-BL SNe suggests that JJEM may be the more favourable explosion mechanism for most Ic-BL SNe and in general most core-collapse SNe (Soker, 2022a).

Furthermore, within the SESNe class, several intermediate events lie between Type I and Type II SNe, including IIb, Ibn and Icn. Type IIb events initially show H-lines that diminish over time, eventually revealing prominent He-features, such as SN 1993J (Woosley et al., 1994). Type Ibn SNe share similarities with Type Ib (lack of H I and Si II features) but exhibit additional characteristics of He-rich circumstellar material (CSM)-ejecta interaction, e.g., SN 2006jc (Pastorello et al., 2007). Similarly, Type Icn SNe resemble typical Type Ic events but manifest additional interaction signatures from carbon- or oxygen-rich CSM-ejecta interaction, as observed in SNe 2019hgp (Gal-Yam et al., 2022) and 2021csp (Perley et al., 2022). Whereas, the recent discovery of transitional events like SN 2022crv, which exhibits characteristics between Types Ib and IIb, further complicates classification within these boundaries (Dong et al., 2023).

The diversity in the observed properties of different types of SNe and SNe within the same class is crucial to understanding how the lives of stars end differently. In addition to distinct progenitor and environment systems, diversity in the nature of the powering source and the different characteristics of underlying powering sources could play a vital role in governing the distinct properties of SNe. Classical Type Ib/c SNe are thought to be mainly governed by the radio-active decay chain  $^{56}\text{Ni} \rightarrow ^{56}\text{Co} \rightarrow ^{56}\text{Fe}$  (RD model, Arnett, 1982; Barbon et al., 1984). Some of the SESNe also have circumstellar material (CSM)-ejecta interaction signatures in their early observations, hence claimed to have contributions from the energy deposition from the CSM interaction (CSMI model), e.g., LSQ13ddu (Clark et al., 2020), SN 2019tsf and SN 2019oys (Sollerman et al., 2020). On the other hand, some of Ib/c SNe with peculiar light curves are claimed to be powered by newly formed millisecond magnetar as a central-engine-based power source (MAG model, Kasen and Bildsten 2010; Woosley 2010) or a combined effect involving both millisecond magnetar and  $^{56}\text{Ni}$ -decay, e.g., SNe 1997ef (Wang et al., 2016), 2005bf (Maeda et al., 2007), 2007ru (Wang et al., 2016), PTF11mnb (Taddia et al., 2018), and 2019cad (Gutiérrez et al., 2021), see also recent study by Hu et al. (2023). In addition, spin-down millisecond magnetar is one of the most favourable models to explain the unique observational properties of most SLSNe-I (Inserra et al., 2013; Nicholl et al., 2017; Dessart, 2019; Gottlieb and Metzger, 2024) and GRB-SNe (Kumar et al., 2024). Additionally, recently Rodríguez et al. (2024) have investigated central-engine-based power sources to explain the light curves of SESNe.

Conversely, it's challenging to explain the doubled peak light curves and post-peak undulations in the light curves of SESNe (mainly SLSNe-I) by considering magnetar as a single powering source (Nicholl et al., 2015; Nicholl and Smartt, 2016). However, some studies suggested that introducing a shock breakout driven by the magnetar can explain the initial peak (Kasen et al., 2016; Liu et al., 2021), and variable thermal energy injection in the ejecta from a centrally-located magnetar can explain the post-peak undulations in the light curves of SESNe (Moriya et al., 2022), see also Zhu et al. (2024). Furthermore, the inclusion of jets as a powering source in addition to the magnetar model is found effective in explaining the light curves (along with their bumps) of most core-collapse SNe, including luminous SNe and SLSNe-I (Soker and Gilkis 2017; Soker 2022c; Gottlieb and Metzger 2024, see Soker 2022d for a review). Additionally, the possibility of the formation of jets in fast-rotating progenitors and observed GRBs originated from such progenitors

also raise the possibility of contributions of jets in powering the GRB-SNe (Corsi and Lazzati, 2021; Soker, 2022d). However, we would like to caution that the magnetar model with the MINIM code (Chatzopoulos et al., 2013) used in the present study does not include the above-mentioned features and is unable to fit the pre-peak bumps and the post-peak undulations.

The present study investigates a sample of 11 SESNe with light curves potentially driven by spin-down millisecond magnetars, employing a unified approach to constrain the physical parameters. Additionally, it examines inter-relationships among the derived parameters and also investigates the distribution of SESNe in multi-dimensional parameter space. The paper is organized as follows: Section 2 provides an overview of the SESNe sample used in this study. Section 3 details the light curve modelling procedures, along with the derived fitting parameters and results. Section 4 presents the linear correlations among SESNe parameters obtained from the light curve analysis and investigates their distribution in reduced dimensionality through Principal Component Analysis. Finally, Section 5 summarizes the key findings.

## 2. Sample

This work investigates millisecond magnetars as powering sources in shaping the light curves of various subtypes of SESNe through light curve modelling. The sample comprises a total of 11 SESNe, which includes 1 Ib (SN 2012au), 1 Ibc (SN 2005bf), 4 Ic (SNe 1997ef, 2007ru, PTF11mnb and 2019cad), 1 relativistic Ic-BL (SN 2012ap), 1 GRB-SN (SN 1998bw), 1 GRB-SLSN (SN 2011kl) and 2 SLSNe-I (SNe 2010kd and 2020ank). This section discusses the motivation behind choosing these specific events and shares some details about these cases.

**SLSNe-I:** The majority of SLSNe-I are explained considering the magnetars as their primary power sources (Nicholl et al., 2017; Yu et al., 2017). From the SLSNe-I category, SN 2010kd (slow-evolving) and SN 2020ank (fast-evolving) are added to the sample because the bolometric light curves of SNe 2010kd and 2020ank are regenerated using the magnetar model under the MINIM code and employing the same assumptions (see Kumar et al. 2020 and Kumar et al. 2021, respectively), which are being used in the present work. Hence, these candidates are the most suitable for the sample from the SLSNe-I category, ensuring coherence and consistency. Furthermore, for SNe 2010kd and 2020ank, in addition to the indication of spin-down millisecond magnetars as power sources from the MINIM-based light-curve modelling, the high UV-peak brightness of both events and the flatter expansion velocity in SN 2010kd suggest a central-engine-based powering mechanism for these objects (Kumar et al., 2020, 2021).

**GRB-SLSN:** To date, SN 2011kl is the only SLSN associated with a ULGRB 111209A, and it is also an intermediate event with a brightness higher than all classical GRB-SNe and lower than SLSNe-I (Greiner et al., 2015; Kann et al., 2019). Previous studies recommended MAG (Greiner et al., 2015; Gompertz and Fruchter, 2017; Kumar et al., 2022, 2024) or MAG+RD (Bersten et al., 2016; Wang et al., 2017b) models to explain the unique properties of SN 2011kl. Whereas, Gao et al. (2016) indicated mass-accreting black as a central engine powering source for SN 2011kl, whereas Lin et al. (2020) proposed the formation of a supermassive magnetar which later collapsed into a black hole. Kumar et al. (2022, 2024) also reproduced the light-curve of SN 2011kl using the MAG model and employing the MINIM code. The signatures of millisecond magnetar as a primary powering source of SN 2011kl, its association with an ULGRB, and intermediate luminosity between SLSNe-I and GRB-SNe make it a promising candidate for the sample.

**GRB-SN:** SN 1998bw is the first and most nearby ( $z = 0.00866$ ) Ic-BL SN found associated with GRB 980425 thus far (Galama et al., 1998; Iwamoto et al., 1998; Wang and Wheeler, 1998; Patat et al., 2001). It was termed a hypernova because its kinetic energy was very high, nearly tenfold higher than that of conventional Type Ic SNe. Additionally, the accompanying GRB 980425 displayed a lower isotropic  $\gamma$ -ray luminosity in comparison to other cosmological LGRBs (Kulkarni et al., 1998). The late-time photometric evolution of SN 1998bw exhibited a faster decline than the decay rate of  $^{56}\text{Co} \rightarrow ^{56}\text{Fe}$ , whereas the late-time spectra lack ejecta-wind interaction signatures (Patat et al., 2001), those disfavour RD and CSMI as dominant power sources. On the other hand, Wang et al. (2017a) and Kumar et al. (2024) proposed MAG+RD and MAG, respectively, as the most suitable models to explain the light curve of SN 1998bw. Given its proximity and extensive observations, SN 1998bw emerges as a compelling addition to the sample from the GRB-SNe family.

**Relativistic Ic-BL SN:** SN 2012ap exhibits mildly relativistic ejecta, with near-peak expansion velocity comparable to SN 1998bw. Although there is no observational signature of association of a GRB with SN 2012ap, it is an interesting object because of its highly relativistic behaviour similar to those of GRB-SNe (Margutti et al., 2014; Chakraborti et al., 2015; Milisavljevic et al., 2015; Liu et al., 2015). Notably, its radio observations designate SN 2012ap as the

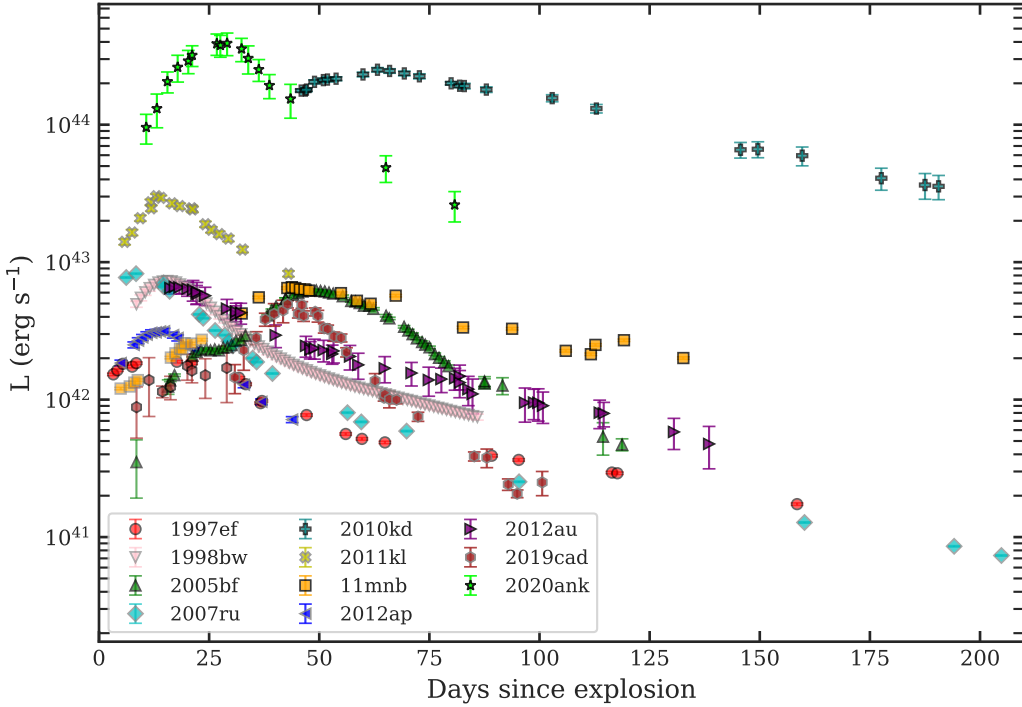


**Figure 1:** Bolometric light curves of the full sample of SESNe used in the present work are shown. Data courtesy: SN 2010kd (Kumar et al., 2020), SN 2020ank (Kumar et al., 2021), SN 2011kl, SN 1998bw, SN 2012ap (Cano et al., 2017, and references therein), SN 1997ef (Iwamoto et al., 2000; Mazzali et al., 2000, 2004), SN 2019cad (Gutiérrez et al., 2021), SN 2005bf (Anupama et al., 2005; Tominaga et al., 2005; Folatelli et al., 2006), SN 2007ru (Sahu et al., 2009), PTF11mnb (Taddia et al., 2018), SN 2012au (Pandey et al., 2021).

least energetic explosion driven by a central engine (Margutti et al., 2014; Chakraborti et al., 2015). Moreover, Kumar et al. (2024) suggested a millisecond magnetar as the primary power source for SN 2012ap, supported by light curve modelling using the MINIM code. The above characteristics make SN 2012ap a good candidate to add to the sample.

**Type Ic SNe:** Within the Type Ic category, the sample includes SNe 1997ef, 2007ru, PTF11mnb and 2019cad, all suggested to be powered by millisecond magnetars in different literature.

**SN 1997ef:** shares high kinetic energy and a broad peak light curve similar to SN 1998bw but distinct from classical Type Ic SNe (Iwamoto et al., 1998; Mazzali et al., 2000, 2004). Based on light curve modelling, Wang et al. (2016) suggested the MAG+RD as the most suitable model for this event.

**SN 2007ru:** exhibits high ejecta expansion velocity and high peak luminosity comparable to SN 1998bw, placing it among the most luminous Type Ic SNe (Sahu et al., 2009). Similar to SN 1997ef, Wang et al. (2016) proposed the MAG+RD model as the optimal choice to trace the bolometric light curve of SN 2007ru.

**PTF11mnb:** displays a double-peak light curve with a fainter first peak followed by a more prominent secondary peak (Taddia et al., 2018), similar to SN 2005bf (Folatelli et al., 2006). In their analysis, Taddia et al. (2018) characterised the first peak using the RD model, while the main/secondary peak was defined using the MAG model. The light curve was also interpreted with a model accounting for a double-peaked  $^{56}\text{Ni}$  distribution (Taddia et al., 2018).

**SN 2019cad:** shows a dual-peak light curve similar to PTF11mnb (Gutiérrez et al., 2021). Therefore, akin to PTF11mnb, the bolometric light curve of SN 2019cad is explained using a double-peaked  $^{56}\text{Ni}$  distribution and a hybrid model which involves tracing the first peak using the RD model and the main peak using the MAG model (Gutiérrez et al., 2021).

**Type Ibc SN:** SN 2005bf exhibits a dual-peak light curve and is claimed a Type Ibc SN with a possible asymmetric ejected envelope (Anupama et al., 2005; Tominaga et al., 2005; Folatelli et al., 2006; Maund et al., 2007; Parrent et al.,

## Magnetar-driven Light Curves of SESNe

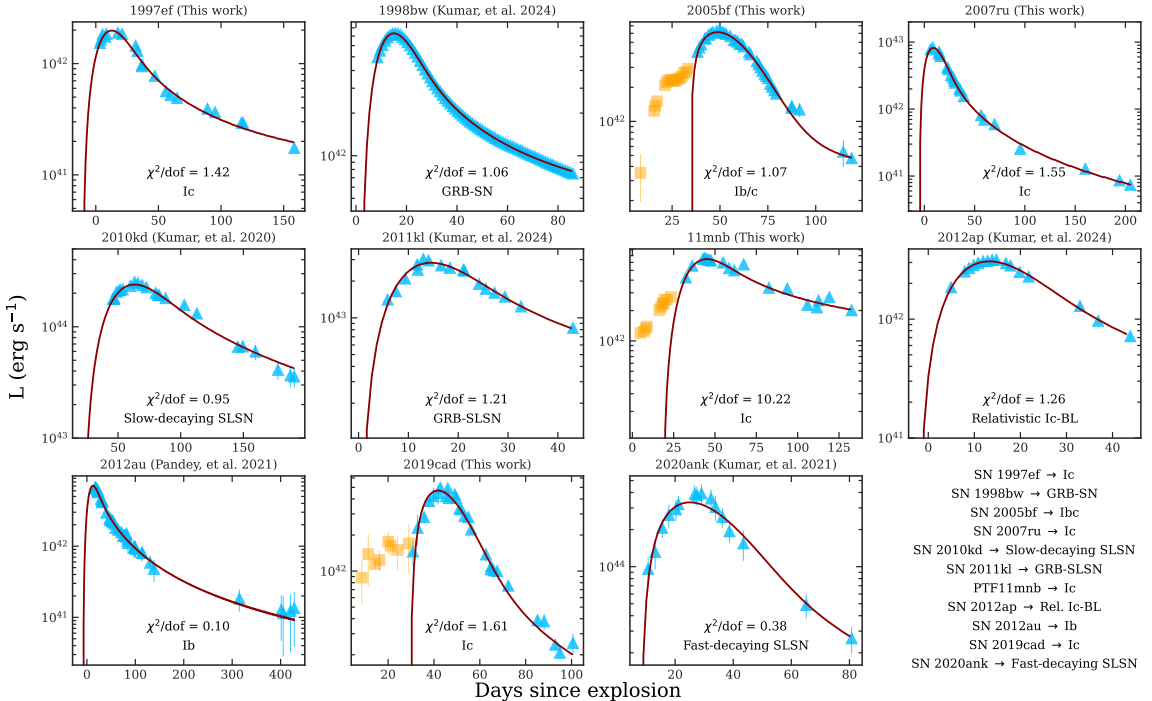


**Figure 2:** Bolometric light curve fittings of 11 SESNe performed utilising the MAG model within the MINIM code (Chatzopoulos et al., 2013) are shown. The light curves of all SESNe within the sample are fitted with low  $\chi^2/\text{dof}$  values (except PTF11mnb, due to highly scattered data). Pre-peak bumps (in orange) in the case of SNe 2005bf, PTF11mnb and 2019cad are masked and not included in the fitting. See Table 1 for estimated fitting parameters.

2007). Its early features indicate it as a type Ic SN; however, the late phase spectral evolution seems similar to Type Ib SNe. Maeda et al. (2007) suggested that the shock heating could power the low-luminous/first peak, whereas a millisecond magnetar may be the primary power source for the secondary/main peak.

**Type Ib SN:** SN 2012au is a very peculiar Type Ib SN, an intermediate event between Ib/c and Ic-BL SNe (Pandey et al., 2021). No CSM interaction signatures were found in the very late-time spectrum of SN 2012au, and a pulsar wind nebula remnant was suggested for this event (Milisavljevic et al., 2018). In addition, this is the only Type Ib SN that is claimed to be driven by a millisecond magnetar based on light-curve (Pandey et al., 2021) and spectral modelling (Omand and Jerkstrand, 2023). These properties prove SN 2012au is an excellent event for the sample.

This study uses this diverse sample of SESNe to investigate the magnetar as a primary central-engine powering source among various subtypes of SESNe. Bolometric light curves were generated only for certain SESNe in the sample, as needed, using the method detailed in Kumar et al. (2024). The bolometric light curves of all the 11 SESNe mentioned above are shown in Figure 1. Data courtesy: SN 2010kd (Kumar et al., 2020), SN 2020ank (Kumar et al., 2021), SN 2011kl, SN 1998bw, SN 2012ap (Cano et al., 2017, and references therein), SN 1997ef (Iwamoto et al., 2000; Mazzali et al., 2000, 2004), SN 2019cad (Gutiérrez et al., 2021), SN 2005bf (Anupama et al., 2005; Tominaga et al., 2005; Folatelli et al., 2006), SN 2007ru (Sahu et al., 2009), PTF11mnb (Taddia et al., 2018), SN 2012au (Pandey et al., 2021). The bolometric light curves for the events within this sample cover a wide range of peak luminosity from lowest peak luminosity  $\sim 2 \times 10^{42} \text{ erg s}^{-1}$  (for SN 1997ef) to highest peak luminosity  $\sim 4 \times 10^{44} \text{ erg s}^{-1}$  (for SN 2020ank).

### 3. Light curve modelling

This work focuses on investigating millisecond magnetars as the primary power source governing the light curves of SESNe and constrains the crucial parameters. To achieve this, MINIM code is used, which is a promising tool to perform the semi-analytical light curve modelling of SESNe (Chatzopoulos et al., 2013), see also (Wheeler et al., 2017; Kumar et al., 2020, 2021; Pandey et al., 2021; Kumar et al., 2022, 2024). MINIM is a robust  $\chi^2$ -minimization

tool implemented in C++ (Chatzopoulos et al., 2013). A comprehensive description of MINIM, including its operational methodology, is detailed in Chatzopoulos et al. (2013).

To probe the underlying power source, MINIM code facilitates the performance of light curve modelling of SNe using numerous models, e.g., RD, CSMI, MAG, and hybrid (CSM+RD) models. However, the present work explores the spin-down millisecond magnetar as a central-engine-based power source for a sample of SESNe; therefore, this study focuses only on the MAG model. For a comprehensive understanding of the MAG model and the underlying assumptions applied in the current study, see Chatzopoulos et al. (2012, 2013).

Under the MAG model, there are six fitting parameters:  $t_i$  (the initial epoch of explosion), magnetar rotational energy ( $E_p$ ), diffusion time scale ( $t_d$ ), spin-down timescale ( $t_p$ ), progenitor radius ( $R_p$ ), and  $V_{\text{exp}}$ . Whereas, other crucial parameters such as initial spin period ( $P_i$ ), magnetic field ( $B$ ), ejecta mass ( $M_{\text{ej}}$ ) and explosion energy of the SN ( $E_{\text{exp}}$ ) can be estimated utilising the above parameters obtained through light curve fitting (e.g.,  $E_p$ ,  $t_p$ ,  $t_d$  and  $V_{\text{exp}}$ ). As outlined in (Chatzopoulos et al., 2012, 2013),  $P_i = \left(\frac{2 \times 10^{50} \text{ erg s}^{-1}}{E_p}\right)^{0.5} \times 10 \text{ ms}$  and  $B = \left(\frac{1.3 \times P_{10}^2}{t_{p,\text{yr}}}\right)^{0.5} \times 10^{14} \text{ G}$ . Furthermore, the values of  $M_{\text{ej}}$  can be computed using equation 1 of Wheeler et al. (2015),  $M_{\text{ej}} \sim \frac{1}{2} \frac{\beta c}{\kappa} V_{\text{exp}} t_d^2$ , adopting  $\beta = 13.8$  and  $\kappa = 0.1 \text{ cm}^2 \text{ g}^{-1}$ , considering half fully-ionized gas, as recommended by Inserra et al. (2013); Wheeler et al. (2015); Wang et al. (2017a). In addition,  $E_{\text{exp}}$  can be estimated using equation 3 of Wheeler et al. (2015),  $E_{\text{SN}} \approx \frac{3}{10} M_{\text{ej}} V_{\text{exp}}^2$ , considering kinetic energy of the SN approximately equals to the explosion energy.

The MAG model within the MINIM code well-explained the light curves of all the SESNe presented here, with  $\chi^2/\text{dof}$  values close to one, except for PTF11mnb ( $\chi^2/\text{dof} = 10.22$ ), potentially due to large scatter in its data. For five SESNe (1997ef, 2005bf, 2007ru, PTF11mnb, and SN 2019cad), the light curve modelling using the MINIM code is conducted independently within this work. In the case of, SNe 2005bf, PTF11mnb and 2019cad, strategically masked the initial/low-luminosity peak (depicted in orange colour in Figure 2) and focused on the light curve modelling solely on the secondary/main peak, as suggested by Maeda et al. (2007), Taddia et al. (2018) and Gutiérrez et al. (2021), respectively. On the other hand, for the rest of six SNe 2010kd (Kumar et al., 2020), 2020ank (Kumar et al., 2021), 2011kl, 1998bw, 2012ap (Kumar et al., 2024), and 2012au (Pandey et al., 2021), the light curve modelling results are directly adopted from existing literature, where the MINIM code was employed to model the light curves, ensuring methodological consistency in this analysis. Nevertheless, only the  $M_{\text{ej}}$  values are recalculated for these cases by incorporating the provided equation and assuming a consistent  $\kappa$  value. It is important to acknowledge that a degree of parameter degeneracy could introduce potential bias in the inferred parameters, as extensively discussed by Chatzopoulos et al. (2013); nevertheless, careful consideration is affirmed in interpreting the results.

The results of the light curve fitting are shown in Figure 2, and the corresponding fitting parameters are listed in Table 1. Table 1 includes only the parameters directly obtained from the light curve modelling ( $E_p$ ,  $t_p$ ,  $t_d$ ,  $R_p$ , and  $V_{\text{exp}}$ ), whereas  $t_i$  is not included due to large uncertainty associated because of masking initial faint peak in some cases. While parameters derived from these fitting parameters, such as  $P_i$ ,  $B$ ,  $M_{\text{ej}}$ , and  $E_{\text{exp}}$  are tabulated in Table 2. In addition, Table 2 also listed peak luminosity ( $L_p$ ), rise time from half-peak to peak luminosity during the pre-peak phase ( $t_{r_{L_p/2}}$ ), and decay time from peak to half-peak luminosity in the post-peak phase ( $t_{d_{L_p/2}}$ ) for SESNe in the sample, that capture the light curve behaviour of SNe around the peak. These parameters were determined via fitting using the Gaussian Process (GP) regression (Rasmussen and Williams, 2005; Bishop, 2006) with a Radial Basis Function (RBF) kernel, offering a more precise fit than spline fitting and replicating the bolometric light curves while naturally providing phase-based uncertainty estimates (Inserra et al., 2018; Kumar and Sharma, 2024). The Python packages `sklearn` and `scipy` were employed for the analysis. For cases lacking pre-peak data near half-peak phases (except for SNe 2011kl, 2019cad, and 2020ank),  $t_{r_{L_p/2}}$  was inferred from the magnetar fitting curve.

As expected, SLSNe 2010kd and 2020ank exhibit  $\approx 10 - 100$  times higher  $L_p$  in comparison to the other SESNe studied here. In addition, slow-evolving SLSN 2010kd shows a longer rise time of approximately 23.7 d, while SNe Ib/c, such as 2005bf and 2007ru, exhibit shorter rise times, around 8-12 d, which suggests a difference in energy injection timescales among these objects. Within the sample used here, SLSNe and Ibc SNe show comparable values of  $V_{\text{exp}}$  ( $\sim 12,000 \text{ km s}^{-1}$ ), while Ic-BL SNe 1998bw and 2012ap, and GRB-SLSN 2011kl, exhibit comparatively higher  $V_{\text{exp}}$  ( $\gtrsim 20,000 \text{ km s}^{-1}$ ). The  $R_p$  varies widely, with SLSNe 2010kd and 2020ank having smaller radii around  $10^{13} \text{ cm}$ , while the progenitor radii of SNe Ib/c, such as PTF11mnb, extend to around  $15 \times 10^{13} \text{ cm}$ . Among SNe Ib/c (2005bf, 2007ru, PTF11mnb, 2012au, and 2019cad; excluding 1997ef), there is consistency in  $P_i$  values around 20 ms, whereas SLSNe 2010kd and 2020ank share the lowest  $P_i$  values around 2.3 ms. On the other hand, SNe Ib/c

**Table 1**

Optimal parameters along with their associated errors provided within the parentheses for 11 SESNe in the sample obtained through the light curve modelling under the MAG model and employing the MINIM code (Chatzopoulos et al., 2013).

object	Type	$E_p^a$ ( $10^{49}$ erg)	$t_d^b$ (d)	$t_p^c$ (d)	$R_p^d$ ( $10^{13}$ cm)	$V_{\text{exp}}^e$ ( $10^3$ km/s)	$\chi^2_{\text{dof}}$	Source
1997ef	Ic	1.29 (0.01)	21.53 (0.21)	18.70 (0.36)	12.42 (1.18)	11.98 (2.38)	1.42	This work
1998bw	GRB-SN	2.67 (0.01)	12.35 (0.07)	9.49 (0.09)	19.26 (0.57)	30.81 (1.43)	1.06	Kumar et al. (2024)
2005bf	Ibc	5.89 (0.11)	26.96 (0.15)	2.98 (0.11)	12.25 (0.64)	10.87 (0.67)	1.07	This work
2007ru	Ic	4.72 (0.01)	15.86 (0.06)	6.01 (0.03)	0.28 (0.03)	14.02 (0.38)	1.55	This work
2010kd	SLSN	337 (6)	35.0 (0.88)	46.85 (2.08)	1.0 (1.25)	11.2 (0.98)	0.95	Kumar et al. (2020)
2011kl	GRB-SLSN	11.87 (0.71)	12.68 (0.32)	12.70 (1.22)	10.26 (3.56)	24.46 (2.46)	1.21	Kumar et al. (2024)
11mnb	Ic	4.61 (0.36)	20.57 (0.41)	37.57 (1.72)	14.81 (0.99)	11.41 (0.35)	10.22	This work
2012ap	Rel. Ic-BL	1.20 (0.01)	16.17 (1.07)	6.71 (0.21)	29.63 (4.35)	21.38 (4.56)	1.26	Kumar et al. (2024)
2012au	Ib	6 (1)	20.83 (2.28)	24.49 (2.12)	0.36 (0.13)	11.66 (0.58)	0.10	Pandey et al. (2021)
2019cad	Ic	4.14 (0.11)	18.22 (0.22)	2.07 (0.08)	0.04 (0.27)	10.10 (0.91)	1.61	This work
2020ank	SLSN	402 (19)	25.01 (0.16)	2.79 (0.35)	0.28 (0.22)	12.27 (0.91)	0.38	Kumar et al. (2021)

<sup>a</sup>  $E_p$ : initial rotational energy of the magnetar. <sup>b</sup>  $t_d$ : diffusion timescale. <sup>c</sup>  $t_p$ : spin-down timescale. <sup>d</sup>  $R_p$ : progenitor star's radius. <sup>e</sup>  $V_{\text{exp}}$ : expansion velocity.

**Table 2**

Light curve parameters for all 11 SESNe in the sample, along with their associated errors (provided in parentheses), estimated using the parameters listed in Table 1 and Gaussian Process (GP) regression fitting on bolometric light curves.

object	Type	$P_i^a$ (ms)	$B^b$ ( $10^{14}$ G)	$M_{\text{ej}}^c$ ( $M_\odot$ )	$E_{\text{exp}}^d$ ( $10^{51}$ erg)	$L_p^e$ ( $10^{42}$ erg/s)	$t_{r_{L_p/2}}^f$ (d)	$t_{d_{L_p/2}}^g$ (d)
1997ef	Ic	39.31 (0.08)	19.83 (0.19)	4.28 (0.94)	3.66 (1.66)	1.93 (0.06)	13.96	21.79 (5.73)
1998bw	GRB-SN	27.38 (0.04)	19.38 (0.09)	3.62 (0.21)	20.50 (2.24)	7.26 (0.03)	7.81	13.80 (0.60)
2005bf	Ibc	18.42 (0.18)	23.29 (0.41)	6.08 (0.20)	4.29 (0.55)	6.23 (0.03)	11.77	21.58 (0.86)
2007ru	Ic	20.58 (0.04)	18.31 (0.05)	2.72 (0.09)	3.19 (0.20)	8.09 (0.20)	8.83	16.24 (1.16)
2010kd	SLSN	2.44 (0.13)	0.78 (0.01)	10.56 (1.46)	4.27 (0.78)	246.38 (3.78)	23.71	49.16 (2.70)
2011kl	GRB-SLSN	12.98 (0.39)	7.95 (0.38)	3.03 (0.46)	10.82 (2.72)	29.22 (1.11)	9.05 (2.01)	13.85 (3.07)
11mnb	Ic	20.82 (0.26)	7.41 (0.17)	3.72 (0.26)	2.89 (0.27)	6.70 (0.14)	16.06	44.87 (8.64)
2012ap	Rel. Ic-BL	40.77 (0.97)	34.34 (0.54)	4.30 (1.49)	11.73 (6.44)	3.13 (0.02)	9.41	19.31 (0.59)
2012au	Ib	18.26 (0.01)	8.05 (0.15)	3.90 (1.05)	3.83 (0.92)	6.74 (0.10)	11.78	23.72 (0.43)
2019cad	Ic	21.97 (0.30)	33.29 (0.67)	2.58 (0.29)	1.57 (0.33)	4.79 (0.15)	11.06 (2.08)	11.41 (1.93)
2020ank	SLSN	2.23 (0.51)	2.91 (0.07)	5.91 (0.51)	3.22 (0.48)	393.23 (8.29)	11.94 (0.81)	11.26 (0.91)

<sup>a</sup>  $P_i$ : initial spin period of the magnetar. <sup>b</sup>  $B$ : magnetic field strength of magnetar. <sup>c</sup>  $M_{\text{ej}}$ : ejected mass. <sup>d</sup>  $E_{\text{exp}}$ : explosion energy of the supernova. <sup>e</sup>  $L_p$ : peak luminosity of bolometric light curve. <sup>f</sup>  $t_{r_{L_p/2}}$ : rise time – the time between half peak luminosity to peak luminosity in the pre-peak phase. <sup>g</sup>  $t_{d_{L_p/2}}$ : decay time – the time between peak luminosity to half peak luminosity in the post-peak phase.

events show higher  $B$  values, with SNe 2005bf and 2012ap exhibiting strengths around  $23 \times 10^{14}$  G and  $34 \times 10^{14}$  G, respectively, while SLSNe 2010kd and 2020ank display comparatively lower values of  $B$  around  $0.8 \times 10^{14}$  G and  $2.9 \times 10^{14}$  G, respectively.

Furthermore, within the sample of SESNe used in the present study, the  $E_{\text{exp}}$  is higher in GRB-SNe (1998bw and 2011kl) and Rel. Ic-BL SN (2012ap), with  $E_{\text{exp}} > 10^{52}$  erg, in contrast to lower values observed in other SESNe, with SN 2019cad with the lowest  $E_{\text{exp}}$  of  $\sim 1.57 \pm 0.33 \times 10^{51}$  erg. However, a detailed study on SN 2019cad by Gutiérrez et al. (2021) suggested  $E_{\text{exp}}$  of  $3.5 \times 10^{51}$  erg for this event. This discrepancy could be because of the different models used to reproduce the light curve of SN 2019cad. As discussed above, among the two popular theoretical mechanisms that explain the explosion of SESNe - delayed neutrino explosion and JJEM - the former can not explain the SNe with  $E_{\text{exp}} \gtrsim 2 \times 10^{51}$  erg (Fryer et al., 2012; Sukhbold et al., 2016; Gogilashvili et al., 2021). All the SESNe in the sample used here show  $E_{\text{exp}} > 2 \times 10^{51}$  erg, indicating JJEM as their possible explosion mechanism and indicating that these SESNe could be driven by jets (see a review by Soker 2022d for details jet-driven core-collapse SNe).

#### 4. Investigating Light Curve Parameters

This section presents the exploratory analysis and dimensionality reduction techniques applied to investigate correlations and dependencies among the parameters of all SESNe in the sample, tabulated in Tables 1 and 2. By

examining these sources in multi-dimensional parameter space, the aim is to uncover underlying relationships and gain deeper insights into their behaviour.

#### 4.1. Correlation Analysis

This section discusses a correlation analysis using Pearson's correlation coefficient to identify potential linear dependencies among the parameters tabulated in Tables 1 and 2, which includes  $R_p$ ,  $M_{ej}$ ,  $P_i$ ,  $B$ ,  $E_{exp}$ ,  $t_{r_{Lp/2}}$ ,  $t_{d_{Lp/2}}$  and  $L_p$ . In the view of the fact that  $M_{ej}$ ,  $P_i$ ,  $B$  and  $E_{exp}$  are computed directly using the other light curve fitting parameters tabulated in Table 1 (except  $R_p$ ) as discussed in Section 3, the parameters  $E_p$ ,  $t_d$ ,  $t_p$ , and  $V_{exp}$  are excluded from the correlation analysis. A heatmap of the correlation matrix is presented in Figure 3.

Parameters  $B - R_p$ ,  $t_{r_{Lp/2}} - M_{ej}$ ,  $t_{d_{Lp/2}} - M_{ej}$  and  $L_p - t_{r_{Lp/2}}$  show the moderate correlations (0.4 to 0.59); and  $t_{r_{Lp/2}} - P_i$ ,  $t_{r_{Lp/2}} - B$ ,  $t_{r_{Lp/2}} - E_{exp}$ ,  $t_{d_{Lp/2}} - B$  and  $L_p - R_p$  present the moderate anti-correlations (-0.4 to -0.59). Whereas,  $P_i - R_p$ ,  $P_i - B$ , and  $E_{exp} - R_p$  show strong correlations (0.6 to 0.79);  $P_i - L_p$  and  $B - L_p$  present strong anti-correlations (-0.6 to -0.79); and  $t_{r_{Lp/2}} - t_{d_{Lp/2}}$  exhibits very strong correlation (0.87). The details about the parameters that present strong correlation or anti-correlation are as follows.

- $t_{r_{Lp/2}} - t_{d_{Lp/2}}$ : A very strong positive correlation (0.87) between  $t_{r_{Lp/2}}$  and  $t_{d_{Lp/2}}$  indicates that SNe with longer rise rates also tend to have extended decay rates, and vice versa. This relationship stems from the dependency of light curve evolution on the diffusion timescale, which depends on ejecta mass, explosion energy, and opacity (Arnett, 1982), see also (Drout et al., 2011; Taddia et al., 2015; Prentice et al., 2016). Typically, SESNe with longer rise times display slower decay times due to larger ejecta mass, opacity and/or lower explosion energy, which results in extended photon diffusion times. Also, SESNe with higher stripped progenitors and higher explosion energies exhibit sharper rise and decay times due to rapid energy release (Taddia et al., 2015; Prentice et al., 2016). The scatter plot of  $t_{r_{Lp/2}}$  vs.  $t_{d_{Lp/2}}$  in this study further supports this linear relationship across SESNe subclasses, see the upper-left panel of Figure 4. SN 2010kd exhibits the highest rise and decay times (it has the highest diffusion time scale and ejecta mass in the sample) whereas SN 1998bw presents the lowest rise and decay times (it contains the lowest diffusion time and among the low ejecta mass SESNe in the sample), see Tables 1 and 2.

- $P_i - B$ : A strong positive correlation between  $P_i$  and  $B$  (0.75) suggests that SESNe within the sample associated with magnetars with higher initial spin periods also exhibits higher magnetic field strengths. The plot presenting  $P_i$  vs.  $B$  in the upper-middle panel of Figure 4 also shows a linear positive relationship between  $P_i$  and  $B$ , though with a significant scatter. Although, as mentioned in Section 3,  $B$  is directly proportional to  $P_i$  and is inversely proportional to  $\sqrt{t_p}$ , which could lead to the linear positive relationship observed between  $B$  and  $P_i$ . Figure 3 of Kumar et al. (2024) also illustrates the  $P_i$  vs.  $B$  relation for different types of transients, including GRB-SNe, SLSNe-I, long GRBs, and short GRBs, showing considerable scatter in  $P_i$  vs.  $B$  even among SNe of the same class (such as in the case of SLSNe-I) and no notable linear relationship can be seen. Thus, the linear relationship between  $P_i$  and  $B$  observed in this study may not be a general trend and could arise from the smaller sample size used in this analysis.
- $P_i - R_p$ : A strong positive correlation (0.7) between  $P_i$  and  $R_p$  suggests that SNe originated from progenitors with larger radii and can also form centrally located newborn magnetars with higher initial spin periods (slower rotating). This could be mainly due to rotational energy constraints and angular momentum distribution within the progenitor star. In progenitors with larger radii, angular momentum is distributed over a more significant volume, generally resulting in a slower core rotation rate and a higher initial spin period (Woosley, 2010; Metzger et al., 2015; Müller et al., 2019). The scatter plot of  $P_i$  vs.  $R_p$  generated in this work (see the upper-right panel of Figure 4) clearly shows a linear relationship between  $P_i$  and  $R_p$ ; SESNe with higher  $P_i$  exhibit higher  $R_p$ , however, with four outliers (SNe 1997ef, 2007ru and 2012au, 2019cad).
- $E_{exp} - R_p$ : A strong positive correlation of 0.65 between  $E_{exp}$  and  $R_p$  suggests that SNe with more extended progenitor tend to have higher explosion energies. The scatter plot between  $E_{exp}$  and  $R_p$  is shown in the lower-left panel of Figure 4, where a positive trend is not clearly visible because of the huge scatter. Contrary, Goldberg et al.

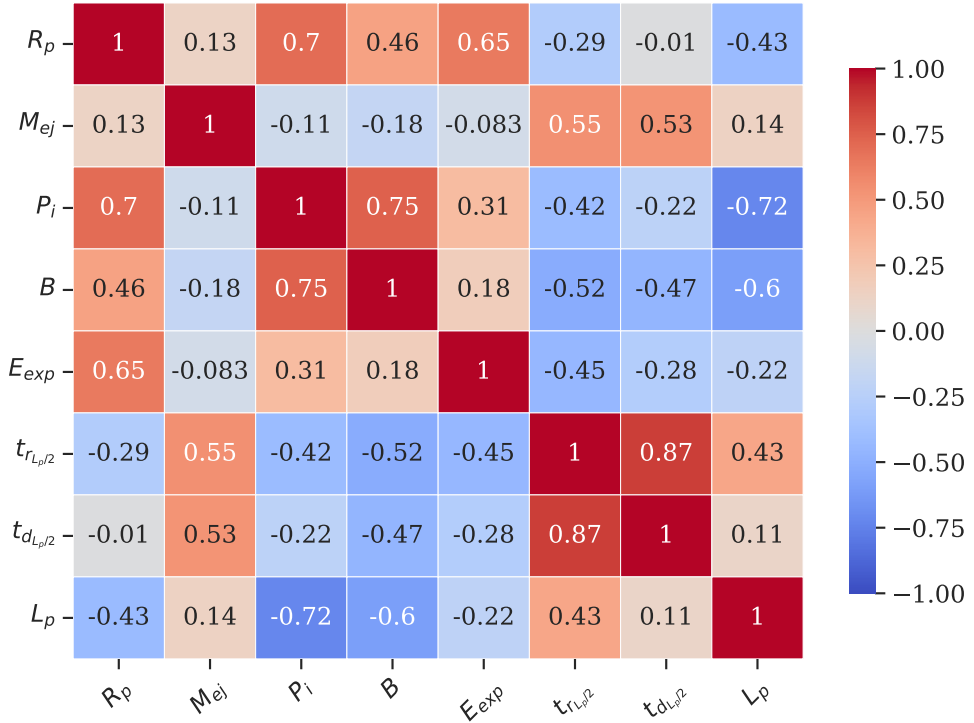


**Figure 3:** Heatmap representation of the correlation matrix among various physical parameters, e.g.,  $R_p$ ,  $M_{ej}$ ,  $P_i$ ,  $B$ ,  $E_{exp}$ ,  $t_{r_{Lp/2}}$ ,  $t_{d_{Lp/2}}$  and  $L_p$ . The heatmap highlights parameter pairs with strong positive correlations in red, suggesting a linear relationship between those parameters. Whereas, parameters with inverse relationships are shown in blue, providing insight into possible anti-correlation.

(2019) demonstrate that the explosion energy of a supernova is inversely proportional to the progenitor radius, whereas it is also influenced by additional factors such as luminosity, nickel mass, and light curve timescales, creating a tricky interdependence that shapes the resulting bolometric light curves of SNe.

- $P_i - L_p$  and  $B - L_p$ : A negative correlation of  $-0.72$  and  $-0.6$  respectively between  $P_i - L_p$  and  $B - L_p$  suggest that supernovae powered by slower-spinning (higher  $P_i$ ) and highly magnetised magnetars tend to have the lower peak luminosities. However, this is not unexpected and follows directly from the relationship  $P_i \propto E_p^{-0.5}$ , where  $E_p$  represents the magnetar's initial rotational energy. In the magnetar model, the supernova light curve is driven by the deposition of this rotational energy into the supernova ejecta. Therefore,  $L_p$  is expected to scale with  $E_p$ . Since  $P_i$  is inversely related to  $E_p$ , this implies that  $L_p$  will also be inversely proportional to  $P_i$ . Similarly, as discussed, the positive correlation between  $B$  and  $P_i$  are positively correlated which results in a negative correlation between  $B$  and  $L_p$ , see also Metzger et al. (2015) for  $P_i$  and  $B$  dependence on  $L_p$  along with other parameters. See the lower middle and right panels of Figure 4 for the scatter plots of  $P_i$  vs.  $L_p$  and  $B$  vs.  $L_p$ , respectively, which appear to exhibit reciprocal behaviours.

## 4.2. Dimensionality Reduction

To further investigate the properties of SESNe based on the parameters derived from the light curve analysis, Principal Component Analysis (PCA, Pearson 1901) is applied to the set of parameters used in the correlation analysis in Section 4.1. PCA reduces the dimensionality of the dataset by transforming a multi-dimensional parameter space into orthogonal principal components (PCs), which are linear combinations of the original parameters. The PCs capture the maximum variance in the dataset while minimizing redundancy, reducing any overlap in the information shared by each component. By identifying the main directions in which the data exhibits the most significant variation, PCA

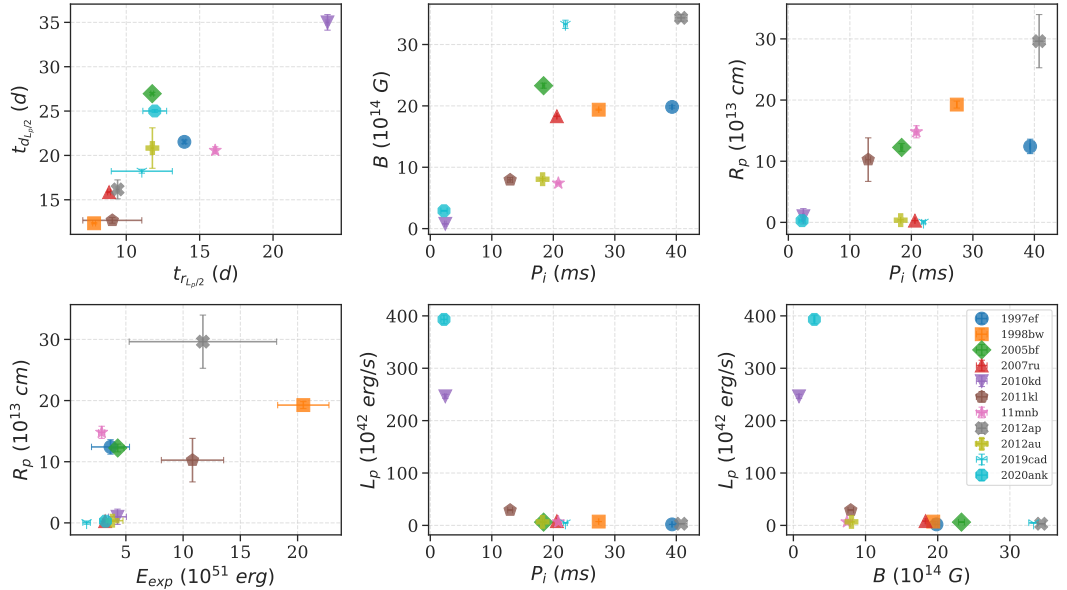


**Figure 4:** Scatter plots for all 11 SESNe in the sample, highlighting parameters with very strong correlations ( $t_{r_{L_p/2}}$  vs.  $t_{d_{L_p/2}}$ ), strong correlations ( $P_i$  vs.  $B$ ,  $P_i$  vs.  $R_p$ , and  $E_{\text{exp}}$  vs.  $R_p$ ), and strong anti-correlations ( $P_i$  vs.  $L_p$  and  $B$  vs.  $L_p$ ).

achieves effective dimensionality reduction, retaining key patterns and relationships within the data. This reduction makes it easier to analyze complex datasets efficiently, maintaining essential features. In the current work, PCA enables clearer visualization and more interpretable insights into different types of SESNe in multi-dimensional parameter space (8 parameters:  $R_p$ ,  $M_{\text{ej}}$ ,  $P_i$ ,  $B$ ,  $E_{\text{exp}}$ ,  $t_{r_{L_p/2}}$ ,  $t_{d_{L_p/2}}$  and  $L_p$ ; corresponds to 8-dimensional parameter space) but with a lower-dimensional, simplified representation (2-dimensional space: PC1 and PC2). The PCA results indicate that the first two principal components (PC1 and PC2) capture approximately 70% of the dataset's variance, with PC1 contributing 47% and PC2 adding 23%. Together, the first four components explain around 90.7% of the variance, providing a solid foundation for visualizing and interpreting the main trends in the data. The positions of 11 SESNe in PC1 - PC2 space are displayed in Figure 5 with circle signs of different colours, and their locations allow for a comparison of parameter distributions, highlighting commonalities and differences among their parameters.

Based on the Loading vs. Parameters inset-plot and the directions of original parameters in PC1 - PC2 space in Figure 5, PC1 seems to have high contributions (loading  $> +0.7$  or  $< -0.7$ ) from  $B$  and  $P_i$  in the negative direction and from  $t_{r_{L_p/2}}$  and  $L_p$  parameters in the positive direction. Whereas, PC1 has a moderate contribution (loading  $+0.4$  to  $0.7$  or  $-0.4$  to  $-0.7$ ) from  $E_{\text{exp}}$  in the negative direction and from  $t_{d_{L_p/2}}$  in the positive direction. On the other hand, PC2 contains high contributions from  $M_{\text{ej}}$  and  $t_{d_{L_p/2}}$ , and moderate contribution from the  $t_{r_{L_p/2}}$  in the negative direction; whereas none of the parameters has a significant contribution in the positive direction. Furthermore,  $R_p$  moderately but equally contributes to the PC1 and PC2 in the negative direction, hence considered neutral (see the inset plot in the upper-right corner of Figure 5). Parameters  $B$ ,  $P_i$ ,  $E_{\text{exp}}$  and  $R_p$ ; and  $M_{\text{ej}}$ ,  $t_{r_{L_p/2}}$  and  $t_{d_{L_p/2}}$  respectively show close clusters, indicating their possible close correlation, whereas  $L_p$  lies in the negative direction of  $P_i$  suggesting their negative correlation, which can also be seen in the correlation analysis presented in Section 4.1.

Among 11 SESNe in PC1 - PC2 plane in Figure 5, SNe 2007ru, 2011kl and 2019cad; and SNe 1997ef, 2005bf and PTF11mnb form relatively compact groups, suggesting that their physical parameters share commonalities. SNe 2007ru, 2011kl and 2019cad share closer values of  $M_{\text{ej}}$ ,  $t_{r_{L_p/2}}$  and  $t_{d_{L_p/2}}$ ; and SNe 1997ef, 2005bf, PTF11mnb present comparatively closer values of  $R_p$ ,  $E_{\text{exp}}$  and  $M_{\text{ej}}$ . On the other hand, SNe 1998bw, 2012ap, 2012au, 2020ank and 2010kd are comparatively isolated and share different locations on the PC1 - PC2 plane, suggesting that these SNe exhibit distinct characteristics. SNe 1998bw and 2012ap share the highest values of  $R_p$  and  $E_{\text{exp}}$ , but their different positions on the PC1 - PC2 plane could arise because of huge differences among their  $B$  values. SN 2012au holds a

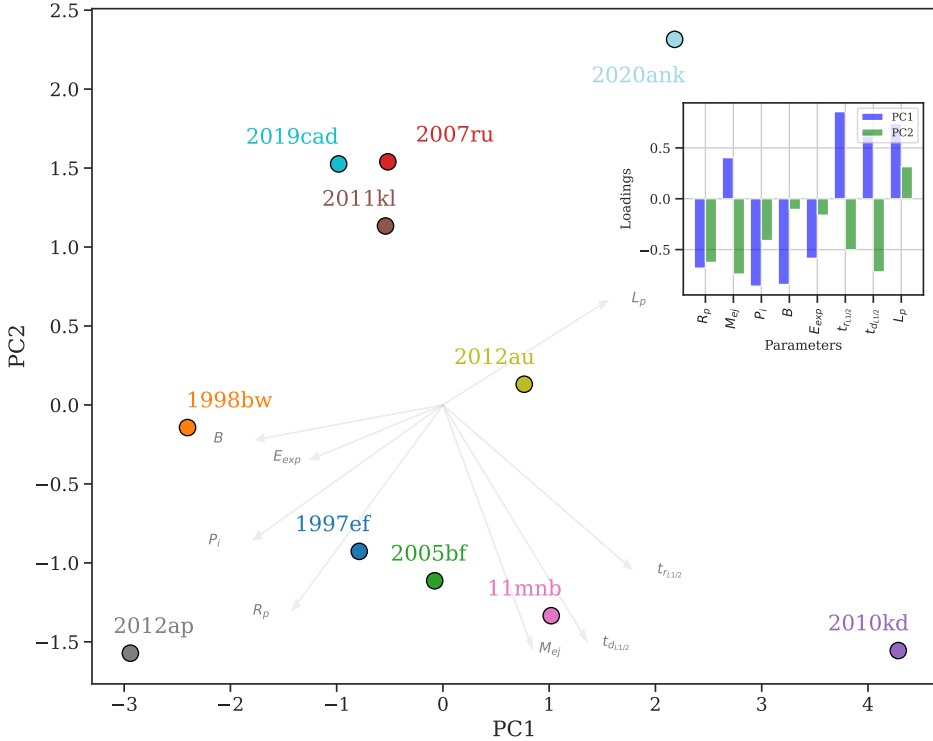


**Figure 5:** PCA reveals that  $\sim 70\%$  of the variance in the dataset is captured by the first two principal components (PC1 - 47% and PC2 - 23%), whereas the first four components collectively explain about 90.7% of the variance in the data, which is sufficient for visualizing and interpreting key trends. The directions of the original 8 parameters used for the PCA (arrows in grey colours) in PC1 - PC2 space and the inset plot with Loadings vs. Parameters in the upper-right corner highlight the contributions of each parameter to PC1 and PC2.

nearly central location on the PC1 - PC2 plane, indicating its balance between different parameters and it seems like an intermediate event among clustered SNe. The locations of both SLSNe 2010kd and 2020ank are well isolated in comparison to other SNe and each other; their lowest values of  $P_i$  and  $B$  place them more isolated from other SESNe in the group, whereas, the highest values of  $M_{ej}$ ,  $t_{r_{Lp/2}}$  and  $t_{d_{Lp/2}}$  of 2010kd than other SESNe and also than those of 2020ank place it isolated than other SESNe and also SLSN 2020ank. Overall, within this limited sample, no clear clustering is observed among SNe of the same SESN subtypes (e.g., Type Ib and SLSNe-I), suggesting that similar SESN types can exhibit distinct physical parameter values. These deviations underscore the complexity and diversity within the population of SESNe, providing key insights into the diverse nature of their powering sources, progenitors and explosion dynamics. However, a study with a more extensive sample is needed to confirm any commonalities or discrepancies among their physical parameters.

## 5. Summary

This work focuses on semi-analytical light curve modelling for a sample of 11 SESNe, considering that these light curves are driven by spin-down millisecond magnetars. The sample includes a diverse set of SESNe subtypes: Type Ib SN 2012u, Ibc SN 2005bf, Ic SNe 1997ef, 2007ru, PTF11mnb, and 2019cad, the relativistic Ic-BL SN 2012ap, GRB-SN 1998bw, GRB-SLSN 2011kl, and superluminous SNe 2010kd and 2020ank. The SNe in this sample span a wide range of peak bolometric luminosities, from approximately  $2 \times 10^{42}$  to  $4 \times 10^{44} \text{ erg s}^{-1}$ , with SN 1997ef showing the lowest and SN 2020ank the highest peak luminosity.

The MAG model under the MINIM code well-regenerates the light curves of all the SESNe in the sample, achieving  $\chi^2/\text{dof}$  values close to one, except for PTF11mnb, which shows significant data scatter. This light curve modelling allows constraining various physical parameters for SNe in the sample, e.g.,  $E_p$ ,  $t_d$ ,  $t_p$ ,  $R_p$ ,  $V_{exp}$ ,  $M_{ej}$ ,  $P_i$ ,  $B$  and  $E_{exp}$ .

In addition,  $L_p$ ,  $t_{r_{L_p/2}}$  and  $t_{d_{L_p/2}}$  are estimated using the GP regression fitting on bolometric light curves of SESNe in the sample.

As anticipated, SLSNe and Ib/c SNe in the sample exhibit lower  $V_{\text{exp}}$  ( $\approx 12,000 \text{ km s}^{-1}$ ) than those of Ic-BL SNe ( $\gtrsim 20,000 \text{ km s}^{-1}$ ). SNe Ib/c in the sample (except SN 1997ef) share comparable  $P_i$  values around 20 ms, whereas SLSNe 2010kd and 2020ank exhibit the lowest  $P_i$  around 2.3 ms. On the other hand, SLSNe 2010kd and 2020ank display the lowest and relativistic Ic-BL SN 2012ap shows the highest values of  $B$  and  $P_i$  values. All the SESNe in the sample (except SN 2019cad) exhibit  $E_{\text{exp}} > 2 \times 10^{51} \text{ erg}$ , suggesting JJEM could be their possible explosion mechanism.

This work further investigates Pearson's correlations among key physical parameters of SESNe derived from light curve analysis. The correlation analysis indicates strong positive correlations between  $t_{r_{L_p/2}}$  and  $t_{d_{L_p/2}}$ ,  $P_i$  and  $B$ ,  $P_i$  and  $R_p$ , and  $E_{\text{exp}}$  and  $R_p$ , as well as strong anti-correlations of  $P_i$  and  $B$  with  $L_p$ . Additionally, the study examines the distribution of SESNe in the PC1 - PC2 space, obtained through PCA-based dimensionality reduction of the multidimensional parameter space of physical parameters of SESNe. The PC1 - PC2 plane from PCA reveals two compact clusters — SNe 2007ru, 2011kl, and 2019cad; and SNe 1997ef, 2005bf, and PTF11mbn — that occupy similar regions in parameter space. While SNe 1998bw, 2012ap, 2012au, 2020ank, and 2010kd appear more isolated, indicating distinct characteristics. This study highlights the unique physical behaviours across SESNe and highlights the value of further exploration of SESNe diversity with an extended sample.

## Data Availability

The publicly available data used in this paper can be accessed through the respective references cited. Additional data supporting this study are available upon request from the corresponding author.

## Acknowledgments

AK is supported by the UK Science and Technology Facilities Council (STFC) Consolidated grant ST/V000853/1. AK is thankful to Dr. Claudia Gutiérrez for sharing the data. AK expresses gratitude to Prof. Jozsef Vinkó and Dr. Kaushal Sharma for providing invaluable insights related to this work. I sincerely thank the anonymous referee for their constructive comments that improved this work. I also acknowledge the invaluable support of NASA's Astrophysics Data System Bibliographic Services.

## References

- Antoni, A., Quataert, E., 2022. Numerical simulations of the random angular momentum in convection: Implications for supergiant collapse to form black holes. *Monthly Notices of the Royal Astronomical Society* 511, 176–197. doi:10.1093/mnras/stab3776, arXiv:2107.09068.
- Anupama, G.C., Sahu, D.K., Deng, J., Nomoto, K., Tominaga, N., Tanaka, M., Mazzali, P.A., Prabhu, T.P., 2005. The Peculiar Type Ib Supernova SN 2005bf: Explosion of a Massive He Star with a Thin Hydrogen Envelope? *The Astrophysical Journal Letters* 631, L125–L128. doi:10.1086/497336, arXiv:astro-ph/0509625.
- Arnett, W.D., 1982. Type I supernovae. I - Analytic solutions for the early part of the light curve. *The Astrophysical Journal* 253, 785–797. doi:10.1086/159681.
- Barbon, R., Cappellaro, E., Turatto, M., 1984. Radioactive decays and supernova light curves. *Astronomy & Astrophysics* 135, 27–31.
- Bear, E., Soker, N., 2025. Identifying a point-symmetric morphology in supernova remnant Cassiopeia A: Explosion by jittering jets. *New Astronomy* 114, 102307. doi:10.1016/j.newast.2024.102307, arXiv:2403.07625.
- Beasor, E.R., Davies, B., Smith, N., van Loon, J.T., Gehrz, R.D., Figer, D.F., 2020. A new mass-loss rate prescription for red supergiants. *Monthly Notices of the Royal Astronomical Society* 492, 5994–6006. doi:10.1093/mnras/staa255, arXiv:2001.07222.
- Bersten, M.C., Benvenuto, O.G., Orellana, M., Nomoto, K., 2016. The Unusual Super-luminous Supernovae SN 2011kl and ASASSN-15lh. *The Astrophysical Journal Letters* 817, L8. doi:10.3847/2041-8205/817/1/L8, arXiv:1601.01021.
- Bethe, H.A., Wilson, J.R., 1985. Revival of a stalled supernova shock by neutrino heating. *The Astrophysical Journal* 295, 14–23. doi:10.1086/163343.
- Bishop, C.M., 2006. Pattern Recognition and Machine Learning. volume 4 of *Information science and statistics*. Springer. URL: <http://www.library.wisc.edu/selectedtoc/bg0137.pdf>, doi:10.1111/1.2819119, arXiv:0-387-31073-8.
- Björklund, R., Sundqvist, J.O., Singh, S.M., Puls, J., Najarro, F., 2023. New predictions for radiation-driven, steady-state mass-loss and wind-momentum from hot, massive stars. III. Updated mass-loss rates for stellar evolution. *Astronomy & Astrophysics* 676, A109. doi:10.1051/0004-6361/202141948, arXiv:2203.08218.
- Boccioli, L., Roberti, L., 2024. The Physics of Core-Collapse Supernovae: Explosion Mechanism and Explosive Nucleosynthesis. *Universe* 10, 148. doi:10.3390/universe10030148, arXiv:2403.12942.
- Bollig, R., Yadav, N., Kresse, D., Janka, H.T., Müller, B., Heger, A., 2021. Self-consistent 3D Supernova Models From -7 Minutes to +7 s: A 1-bethe Explosion of a  $19 M_\odot$  Progenitor. *The Astrophysical Journal* 915, 28. doi:10.3847/1538-4357/abf82e, arXiv:2010.10506.

- Bonanos, A.Z., Tramper, F., de Wit, S., Christodoulou, E., Muñoz Sanchez, G., Antoniadis, K., Athanasiou, S., Maravelias, G., Yang, M., Zapartas, E., 2024. Investigating episodic mass loss in evolved massive stars. I. Spectroscopy of dusty massive stars in ten southern galaxies. *Astronomy & Astrophysics* 686, A77. doi:10.1051/0004-6361/202348527, arXiv:2312.04626.
- Burrows, A., Radice, D., Vartanyan, D., Nagakura, H., Skinner, M.A., Dolence, J.C., 2020. The overarching framework of core-collapse supernova explosions as revealed by 3D FORNAX simulations. *Monthly Notices of the Royal Astronomical Society* 491, 2715–2735. doi:10.1093/mnras/stz3223, arXiv:1909.04152.
- Burrows, A., Vartanyan, D., 2021. Core-collapse supernova explosion theory. *Nature* 589, 29–39. doi:10.1038/s41586-020-03059-w, arXiv:2009.14157.
- Cano, Z., Wang, S.Q., Dai, Z.G., Wu, X.F., 2017. The Observer's Guide to the Gamma-Ray Burst Supernova Connection. *Advances in Astronomy* 2017, 8929054. doi:10.1155/2017/8929054, arXiv:1604.03549.
- Chakraborti, S., Soderberg, A., Chomiuk, L., Kamble, A., Yadav, N., Ray, A., Hurley, K., Margutti, R., Milisavljevic, D., Bietenholz, M., Brunthaler, A., Pignata, G., Pian, E., Mazzali, P., Fransson, C., Bartel, N., Hamuy, M., Levesque, E., MacFadyen, A., Dittmann, J., Krauss, M., Briggs, M.S., Connaughton, V., Yamaoka, K., Takahashi, T., Ohno, M., Fukazawa, Y., Tashiro, M., Terada, Y., Murakami, T., Goldsten, J., Barthelmy, S., Gehrels, N., Cummings, J., Krimm, H., Palmer, D., Golenetskii, S., Aptekar, R., Frederiks, D., Svinkin, D., Cline, T., Mitrofanov, I.G., Golovin, D., Litvak, M.L., Sanin, A.B., Boynton, W., Fellows, C., Harshman, K., Enos, H., von Kienlin, A., Rau, A., Zhang, X., Savchenko, V., 2015. A Missing-link in the Supernova-GRB Connection: The Case of SN 2012ap. *The Astrophysical Journal* 805, 187. doi:10.1088/0004-637X/805/2/187, arXiv:1402.6336.
- Chatzopoulos, E., Wheeler, J.C., Vinko, J., 2012. Generalized Semi-analytical Models of Supernova Light Curves. *The Astrophysical Journal* 746, 121. doi:10.1088/0004-637X/746/2/121, arXiv:1111.5237.
- Chatzopoulos, E., Wheeler, J.C., Vinko, J., Horvath, Z.L., Nagy, A., 2013. Analytical Light Curve Models of Superluminous Supernovae:  $\chi^2$ -minimization of Parameter Fits. *The Astrophysical Journal* 773, 76. doi:10.1088/0004-637X/773/1/76, arXiv:1306.3447.
- Clark, P., Maguire, K., Inserra, C., Prentice, S., Smartt, S.J., Contreras, C., Hossenizadeh, G., Hsiao, E.Y., Kankare, E., Kasliwal, M., Nugent, P., Shahbandeh, M., Baltay, C., Rabinowitz, D., Arcavi, I., Ashall, C., Burns, C.R., Callis, E., Chen, T.W., Diamond, T., Fraser, M., Howell, D.A., Karamehmetoglu, E., Kotak, R., Lyman, J., Morrell, N., Phillips, M., Pignata, G., Pursiainen, M., Sollerman, J., Stritzinger, M., Sullivan, M., Young, D., 2020. LSQ13ddu: a rapidly evolving stripped-envelope supernova with early circumstellar interaction signatures. *Monthly Notices of the Royal Astronomical Society* 492, 2208–2228. doi:10.1093/mnras/stz3598, arXiv:1912.05986.
- Conti, P.S., 1975. On the relationship between Of and WR stars. *Memoires of the Societe Royale des Sciences de Liege* 9, 193–212.
- Corsi, A., Lazzati, D., 2021. Gamma-ray burst jets in supernovae. *New Astronomy Reviews* 92, 101614. doi:10.1016/j.newar.2021.101614.
- Curé, M., Araya, I., 2023. Radiation-Driven Wind Hydrodynamics of Massive Stars: A Review. *Galaxies* 11, 68. doi:10.3390/galaxies11030068, arXiv:2305.11666.
- Dessart, L., 2019. Simulations of light curves and spectra for superluminous Type Ic supernovae powered by magnetars. *Astronomy & Astrophysics* 621, A141. doi:10.1051/0004-6361/201834535, arXiv:1812.03749.
- Dong, Y., Valenti, S., Ashall, C., Williamson, M., Sand, D.J., Van Dyk, S.D., Jha, S.W., Lundquist, M., Modjaz, M., Andrews, J.E., Jencson, J.E., Hosseinzadeh, G., Pearson, J., Kwok, L.A., Boland, T., Hsiao, E.Y., Smith, N., Elias-Rosa, N., Srivastav, S., Smartt, S., Fulton, M., Zheng, W., Brink, T.G., Filippenko, A.V., Shahbandeh, M., Bostroem, K.A., Hoang, E., Janzen, D., Mehta, D., Meza, N., Shrestha, M., Wyatt, S., Auchettl, K., Burns, C.R., Farah, J., Galbany, L., Padilla Gonzalez, E., Haislip, J., Hinkle, J.T., Howell, D.A., De Jaeger, T., Kouprianov, V., Kumar, S., Lu, J., McCully, C., Moran, S., Morrell, N., Newsome, M., Pellegrino, C., Polin, A., Reichart, D.E., Shappee, B.J., Stritzinger, M.D., Terreran, G., Tucker, M.A., 2023. SN 2022crv: IIb, Or Not IIb: That is the Question. arXiv e-prints , arXiv:2309.09433doi:10.48550/arXiv.2309.09433, arXiv:2309.09433.
- Drout, M.R., Götberg, Y., Ludwig, B.A., Groh, J.H., de Mink, S.E., O'Grady, A.J.G., Smith, N., 2023. An observed population of intermediate-mass helium stars that have been stripped in binaries. *Science* 382, 1287–1291. doi:10.1126/science.adc4970, arXiv:2307.00061.
- Drout, M.R., Soderberg, A.M., Gal-Yam, A., Cenko, S.B., Fox, D.B., Leonard, D.C., Sand, D.J., Moon, D.S., Arcavi, I., Green, Y., 2011. The First Systematic Study of Type Ibc Supernova Multi-band Light Curves. *The Astrophysical Journal* 741, 97. doi:10.1088/0004-637X/741/2/97, arXiv:1011.4959.
- Filippenko, A.V., 1997. Optical Spectra of Supernovae. *Annual Review of Astron and Astrophys* 35, 309–355. doi:10.1146/annurev.astro.35.1.309.
- Folatelli, G., Contreras, C., Phillips, M.M., Woosley, S.E., Blinnikov, S., Morrell, N., Suntzeff, N.B., Lee, B.L., Hamuy, M., González, S., Krzeminski, W., Roth, M., Li, W., Filippenko, A.V., Foley, R.J., Freedman, W.L., Madore, B.F., Persson, S.E., Murphy, D., Boissier, S., Galaz, G., González, L., McCarthy, P.J., McWilliam, A., Pych, W., 2006. SN 2005bf: A Possible Transition Event between Type Ib/c Supernovae and Gamma-Ray Bursts. *The Astrophysical Journal* 641, 1039–1050. doi:10.1086/500531, arXiv:astro-ph/0509731.
- Fryer, C.L., Belczynski, K., Wiktorowicz, G., Dominik, M., Kalogera, V., Holz, D.E., 2012. Compact Remnant Mass Function: Dependence on the Explosion Mechanism and Metallicity. *The Astrophysical Journal* 749, 91. doi:10.1088/0004-637X/749/1/91, arXiv:1110.1726.
- Gal-Yam, A., 2017. Observational and Physical Classification of Supernovae, in: Alsabti, A.W., Murdin, P. (Eds.), *Handbook of Supernovae*, p. 195. doi:10.1007/978-3-319-21846-5\_35.
- Gal-Yam, A., 2019. The Most Luminous Supernovae. *Annual Review of Astron and Astrophys* 57, 305–333. doi:10.1146/annurev-astro-081817-051819, arXiv:1812.01428.
- Gal-Yam, A., Bruch, R., Schulze, S., Yang, Y., Perley, D.A., Irani, I., Sollerman, J., Kool, E.C., Soumagnac, M.T., Yaron, O., Strotjohann, N.L., Zimmerman, E., Barbarino, C., Kulkarni, S.R., Kasliwal, M.M., De, K., Yao, Y., Fremling, C., Yan, L., Ofek, E.O., Fransson, C., Filippenko, A.V., Zheng, W., Brink, T.G., Copperwheat, C.M., Foley, R.J., Brown, J., Siebert, M., Leloudas, G., Cabrera-Lavers, A.L., Garcia-Alvarez, D., Marante-Barreto, A., Frederick, S., Hung, T., Wheeler, J.C., Vinkó, J., Thomas, B.P., Graham, M.J., Duev, D.A., Drake, A.J., Dekany, R., Bellm, E.C., Rusholme, B., Shupe, D.L., Andreoni, I., Sharma, Y., Riddle, R., van Roestel, J., Knezevic, N., 2022. A WC/WO star exploding within an expanding carbon-oxygen-neon nebula. *Nature* 601, 201–204. doi:10.1038/s41586-021-04155-1, arXiv:2111.12435.

- Galama, T.J., Vreeswijk, P.M., van Paradijs, J., Kouveliotou, C., Augusteijn, T., Böhnhardt, H., Brewer, J.P., Doublier, V., Gonzalez, J.F., Leibundgut, B., Lidman, C., Hainaut, O.R., Patat, F., Heise, J., in't Zand, J., Hurley, K., Groot, P.J., Strom, R.G., Mazzali, P.A., Iwamoto, K., Nomoto, K., Umeda, H., Nakamura, T., Young, T.R., Suzuki, T., Shigeyama, T., Kosut, T., Kippen, M., Robinson, C., de Wildt, P., Wijers, R.A.M.J., Tanvir, N., Greiner, J., Pian, E., Palazzi, E., Frontera, F., Masetti, N., Nicastro, L., Feroci, M., Costa, E., Piro, L., Peterson, B.A., Tinney, C., Boyle, B., Cannon, R., Stathakis, R., Sadler, E., Begam, M.C., Ianna, P., 1998. An unusual supernova in the error box of the  $\gamma$ -ray burst of 25 April 1998. *Nature* 395, 670–672. doi:10.1038/27150, arXiv:astro-ph/9806175.
- Gao, H., Lei, W.H., You, Z.Q., Xie, W., 2016. The Black Hole Central Engine for Ultra-long Gamma-Ray Burst 111209A and Its Associated Supernova 2011kl. *The Astrophysical Journal* 826, 141. doi:10.3847/0004-637X/826/2/141, arXiv:1605.04660.
- Georgy, C., Meynet, G., Walder, R., Folini, D., Maeder, A., 2009. The different progenitors of type Ib, Ic SNe, and of GRB. *Astronomy & Astrophysics* 502, 611–622. doi:10.1051/0004-6361/200811339, arXiv:0906.2284.
- Gilkis, A., Soker, N., 2015. Implications of Turbulence for Jets in Core-collapse Supernova Explosions. *The Astrophysical Journal* 806, 28. doi:10.1088/0004-637X/806/1/28, arXiv:1412.4984.
- Gilkis, A., Vink, J.S., Eldridge, J.J., Tout, C.A., 2019. Effects of winds on the leftover hydrogen in massive stars following Roche lobe overflow. *Monthly Notices of the Royal Astronomical Society* 486, 4451–4462. doi:10.1093/mnras/stz1134, arXiv:1904.09221.
- Gogilashvili, M., Murphy, J.W., Mabanta, Q., 2021. Explosion energies for core-collapse supernovae I: analytic, spherically symmetric solutions. *Monthly Notices of the Royal Astronomical Society* 500, 5393–5407. doi:10.1093/mnras/staa3546, arXiv:2007.06087.
- Goldberg, J.A., Bildsten, L., Paxton, B., 2019. Inferring Explosion Properties from Type II-Plateau Supernova Light Curves. *The Astrophysical Journal* 879, 3. doi:10.3847/1538-4357/ab22b6, arXiv:1903.09114.
- Gomez, S., Nicholl, M., Berger, E., Blanchard, P.K., Villar, V.A., Rest, S., Hosseinzadeh, G., Aamer, A., Ajay, Y., Athukoralalage, W., Coulter, D.C., Eftekhari, T., Fiore, A., Franz, N., Fox, O., Gagliano, A., Hiramatsu, D., Howell, D.A., Hsu, B., Karmen, M., Siebert, M.R., Könyves-Tóth, R., Kumar, H., McCully, C., Pellegrino, C., Pierel, J., Rest, A., Wang, Q., 2024. The Type I Superluminous Supernova Catalog I: Light curve properties, models, and catalog description. *Monthly Notices of the Royal Astronomical Society* doi:10.1093/mnras/stae2270, arXiv:2407.07946.
- Gompertz, B., Fruchter, A., 2017. Magnetars in Ultra-Long Gamma-Ray Bursts and GRB 111209A. *The Astrophysical Journal* 839, 49. doi:10.3847/1538-4357/aa6629, arXiv:1702.05507.
- Gottlieb, O., Metzger, B.D., 2024. Late Jets, Early Sparks: Illuminating the Premaximum Bumps in Superluminous Supernovae. *The Astrophysical Journal Letters* 974, L9. doi:10.3847/2041-8213/ad7d82, arXiv:2407.20348.
- Greiner, J., Mazzali, P.A., Kann, D.A., Krühler, T., Pian, E., Prentice, S., Olivares E., F., Rossi, A., Klose, S., Taubenberger, S., Knust, F., Afonso, P.M.J., Ashall, C., Bolmer, J., Delvaux, C., Diehl, R., Elliott, J., Filgas, R., Fynbo, J.P.U., Graham, J.F., Guelbenzu, A.N., Kobayashi, S., Leloudas, G., Savaglio, S., Schady, P., Schmidl, S., Schweyer, T., Sudilovsky, V., Tanga, M., Updike, A.C., van Eerten, H., Varela, K., 2015. A very luminous magnetar-powered supernova associated with an ultra-long  $\gamma$ -ray burst. *Nature* 523, 189–192. doi:10.1038/nature14579, arXiv:1509.03279.
- Gutiérrez, C.P., Bersten, M.C., Orellana, M., Pastorello, A., Ertini, K., Folatelli, G., Pignata, G., Anderson, J.P., Smartt, S., Sullivan, M., Pursiainen, M., Inserra, C., Elias-Rosa, N., Fraser, M., Kankare, E., Moran, S., Reguitti, A., Reynolds, T.M., Stritzinger, M., Burke, J., Frohmaier, C., Galbany, L., Hiramatsu, D., Howell, D.A., Kuncarayakti, H., Mattila, S., Müller-Bravo, T., Pellegrino, C., Smith, M., 2021. The double-peaked Type Ic supernova 2019cad: another SN 2005bf-like object. *Monthly Notices of the Royal Astronomical Society* 504, 4907–4922. doi:10.1093/mnras/stab1009, arXiv:2104.03723.
- Heger, A., Fryer, C.L., Woosley, S.E., Langer, N., Hartmann, D.H., 2003. How Massive Single Stars End Their Life. *The Astrophysical Journal* 591, 288–300. doi:10.1086/375341, arXiv:astro-ph/0212469.
- Hu, R.C., Zhu, J.P., Qin, Y., Shao, Y., Zhang, B., Yu, Y.W., Liang, E.W., Liu, L.D., Wang, B., Shu, X.W., Liu, J.F., 2023. Formation of Fast-spinning Neutron Stars in Close Binaries and Magnetar-driven Stripped-envelope Supernovae. *arXiv e-prints*, arXiv:2301.06402doi:10.48550/arXiv.2301.06402, arXiv:2301.06402.
- Inserra, C., 2019. Observational properties of extreme supernovae. *Nature Astronomy* 3, 697–705. doi:10.1038/s41550-019-0854-4, arXiv:1908.02314.
- Inserra, C., Prajs, S., Gutierrez, C.P., Angus, C., Smith, M., Sullivan, M., 2018. A Statistical Approach to Identify Superluminous Supernovae and Probe Their Diversity. *The Astrophysical Journal* 854, 175. doi:10.3847/1538-4357/aaaaaa, arXiv:1711.03787.
- Inserra, C., Smartt, S.J., Jerkstrand, A., Valenti, S., Fraser, M., Wright, D., Smith, K., Chen, T.W., Kotak, R., Pastorello, A., Nicholl, M., Bresolin, F., Kudritzki, R.P., Benetti, S., Botticella, M.T., Burgett, W.S., Chambers, K.C., Ergon, M., Flewelling, H., Fynbo, J.P.U., Geier, S., Hodapp, K.W., Howell, D.A., Huber, M., Kaiser, N., Leloudas, G., Magill, L., Magnier, E.A., McCrum, M.G., Metcalfe, N., Price, P.A., Rest, A., Sollerman, J., Sweeney, W., Taddia, F., Taubenberger, S., Tonry, J.L., Wainscoat, R.J., Waters, C., Young, D., 2013. Super-luminous Type Ic Supernovae: Catching a Magnetar by the Tail. *The Astrophysical Journal* 770, 128. doi:10.1088/0004-637X/770/2/128, arXiv:1304.3320.
- Iwamoto, K., Mazzali, P.A., Nomoto, K., Umeda, H., Nakamura, T., Patat, F., Danziger, I.J., Young, T.R., Suzuki, T., Shigeyama, T., Augusteijn, T., Doublier, V., Gonzalez, J.F., Boehnhardt, H., Brewer, J., Hainaut, O.R., Lidman, C., Leibundgut, B., Cappellaro, E., Turatto, M., Galama, T.J., Vreeswijk, P.M., Kouveliotou, C., van Paradijs, J., Pian, E., Palazzi, E., Frontera, F., 1998. A hypernova model for the supernova associated with the  $\gamma$ -ray burst of 25 April 1998. *Nature* 395, 672–674. doi:10.1038/27155, arXiv:astro-ph/9806382.
- Iwamoto, K., Nakamura, T., Nomoto, K., Mazzali, P.A., Danziger, I.J., Garnavich, P., Kirshner, R., Jha, S., Balam, D., Thorstensen, J., 2000. The Peculiar Type IC Supernova 1997EF: Another Hypernova. *The Astrophysical Journal* 534, 660–669. doi:10.1086/308761, arXiv:astro-ph/9807060.
- Janka, H.T., Melson, T., Summa, A., 2016. Physics of Core-Collapse Supernovae in Three Dimensions: A Sneak Preview. *Annual Review of Nuclear and Particle Science* 66, 341–375. doi:10.1146/annurev-nucl-102115-044747, arXiv:1602.05576.
- Kann, D.A., Schady, P., Olivares E., F., Klose, S., Rossi, A., Perley, D.A., Krühler, T., Greiner, J., Nicuesa Guelbenzu, A., Elliott, J., Knust, F., Filgas, R., Pian, E., Mazzali, P., Fynbo, J.P.U., Leloudas, G., Afonso, P.M.J., Delvaux, C., Graham, J.F., Rau, A., Schmidl, S., Schulze, S., Tanga, M., Updike, A.C., Varela, K., 2019. Highly luminous supernovae associated with gamma-ray bursts. I. GRB 111209A/SN 2011kl in the

- context of stripped-envelope and superluminous supernovae. *Astronomy & Astrophysics* 624, A143. doi:10.1051/0004-6361/201629162, arXiv:1606.06791.
- Kasen, D., Bildsten, L., 2010. Supernova Light Curves Powered by Young Magnetars. *The Astrophysical Journal* 717, 245–249. doi:10.1088/0004-637X/717/1/245, arXiv:0911.0680.
- Kasen, D., Metzger, B.D., Bildsten, L., 2016. Magnetar-driven Shock Breakout and Double-peaked Supernova Light Curves. *The Astrophysical Journal* 821, 36. doi:10.3847/0004-637X/821/1/36, arXiv:1507.03645.
- Kulkarni, S.R., Frail, D.A., Wieringa, M.H., Ekers, R.D., Sadler, E.M., Wark, R.M., Higdon, J.L., Phinney, E.S., Bloom, J.S., 1998. Radio emission from the unusual supernova 1998bw and its association with the  $\gamma$ -ray burst of 25 April 1998. *Nature* 395, 663–669. doi:10.1038/27139.
- Kumar, A., Kumar, B., Pandey, S.B., Sahu, D.K., Singh, A., Anupama, G.C., Aryan, A., Gupta, R., Dutta, A., Misra, K., 2021. SN 2020ank: a bright and fast-evolving H-deficient superluminous supernova. *Monthly Notices of the Royal Astronomical Society* 502, 1678–1693. doi:10.1093/mnras/staa4047, arXiv:2012.15251.
- Kumar, A., Pandey, S.B., Gupta, R., Aryan, A., Ror, A.K., Sharma, S., Brahme, N., 2022. Tale of GRB 171010A/SN 2017htp and GRB 171205A/SN 2017iuk: Magnetar origin? *New Astronomy* 97, 101889. doi:10.1016/j.newast.2022.101889, arXiv:2206.00950.
- Kumar, A., Pandey, S.B., Konyves-Toth, R., Staten, R., Vinko, J., Wheeler, J.C., Zheng, W., Filippenko, A.V., Kehoe, R., Quimby, R., Fang, Y., Akerlof, C., McKay, T.A., Chatzopoulos, E., Thomas, B.P., Dhungana, G., Aryan, A., Dastidar, R., Gangopadhyay, A., Gupta, R., Misra, K., Kumar, B., Brahme, N., Buckley, D., 2020. SN 2010kd: Photometric and Spectroscopic Analysis of a Slow-decaying Superluminous Supernova. *The Astrophysical Journal* 892, 28. doi:10.3847/1538-4357/ab737b, arXiv:2002.04201.
- Kumar, A., Sharma, K., 2024. Light Curve Properties of Gamma-Ray Burst Associated Supernovae. arXiv e-prints, arXiv:2411.13242 doi:10.48550/arXiv.2411.13242, arXiv:2411.13242.
- Kumar, A., Sharma, K., Vinkó, J., Steeghs, D., Gompertz, B., Lyman, J., Dastidar, R., Singh, A., Ackley, K., Pursiainen, M., 2024. Magnetars as powering sources of gamma-ray burst associated supernovae, and unsupervised clustering of cosmic explosions. *Monthly Notices of the Royal Astronomical Society* 531, 3297–3309. doi:10.1093/mnras/stae901, arXiv:2403.18076.
- Levesque, E.M., Soderberg, A.M., Foley, R.J., Berger, E., Kewley, L.J., Chakraborti, S., Ray, A., Torres, M.A.P., Challis, P., Kirshner, R.P., Barthelmy, S.D., Bietenholz, M.F., Chandra, P., Chaplin, V., Chevalier, R.A., Chugai, N., Connaughton, V., Copete, A., Fox, O., Fransson, C., Grindlay, J.E., Hamuy, M.A., Milne, P.A., Pignata, G., Stritzinger, M.D., Wieringa, M.H., 2010. The High-metallicity Explosion Environment of the Relativistic Supernova 2009bb. *The Astrophysical Journal Letters* 709, L26–L31. doi:10.1088/2041-8205/709/1/L26, arXiv:0908.2818.
- Lin, J., Lu, R.J., Lin, D.B., Wang, X.G., 2020. GRB 111209A/SN 2011kl: Collapse of a Supramassive Magnetar with r-mode Oscillation and Fallback Accretion onto a Newborn Black Hole. *The Astrophysical Journal* 895, 46. doi:10.3847/1538-4357/ab88a7, arXiv:2004.05514.
- Liu, L.D., Gao, H., Wang, X.F., Yang, S., 2021. Magnetar-driven Shock Breakout Revisited and Implications for Double-peaked Type I Superluminous Supernovae. *The Astrophysical Journal* 911, 142. doi:10.3847/1538-4357/abf042, arXiv:2103.09971.
- Liu, Z., Zhao, X.L., Huang, F., Wang, X.F., Zhang, T.M., Chen, J.C., Zhang, T.J., 2015. Optical observations of the broad-lined type Ic supernova SN 2012ap. *Research in Astronomy and Astrophysics* 15, 225–236. doi:10.1088/1674-4527/15/2/007.
- Lyman, J.D., Bersier, D., James, P.A., Mazzali, P.A., Eldridge, J.J., Fraser, M., Pian, E., 2016. Bolometric light curves and explosion parameters of 38 stripped-envelope core-collapse supernovae. *Monthly Notices of the Royal Astronomical Society* 457, 328–350. doi:10.1093/mnras/stv2983, arXiv:1406.3667.
- Maeda, K., Mazzali, P.A., Deng, J., Nomoto, K., Yoshii, Y., Tomita, H., Kobayashi, Y., 2003. A Two-Component Model for the Light Curves of Hypernovae. *The Astrophysical Journal* 593, 931–940. doi:10.1086/376591, arXiv:astro-ph/0305182.
- Maeda, K., Tanaka, M., Nomoto, K., Tominaga, N., Kawabata, K., Mazzali, P.A., Umeda, H., Suzuki, T., Hattori, T., 2007. The Unique Type Ib Supernova 2005bf at Nebular Phases: A Possible Birth Event of a Strongly Magnetized Neutron Star. *The Astrophysical Journal* 666, 1069–1082. doi:10.1086/520054, arXiv:0705.2713.
- Margutti, R., Milisavljevic, D., Soderberg, A.M., Guidorzi, C., Morsony, B.J., Sanders, N., Chakraborti, S., Ray, A., Kamble, A., Drout, M., Parrent, J., Zauderer, A., Chomiuk, L., 2014. Relativistic Supernovae have Shorter-lived Central Engines or More Extended Progenitors: The Case of SN 2012ap. *The Astrophysical Journal* 797, 107. doi:10.1088/0004-637X/797/2/107, arXiv:1402.6344.
- Maund, J.R., Wheeler, J.C., Patat, F., Baade, D., Wang, L., Höflich, P., 2007. Spectropolarimetry of the Type Ib/c SN 2005bf. *Monthly Notices of the Royal Astronomical Society* 381, 201–210. doi:10.1111/j.1365-2966.2007.12230.x, arXiv:0707.2237.
- Mazzali, P.A., Deng, J., Maeda, K., Nomoto, K., Filippenko, A.V., Matheson, T., 2004. Properties of Two Hypernovae Entering the Nebular Phase: SN 1997ef and SN 1997dq. *The Astrophysical Journal* 614, 858–863. doi:10.1086/423888, arXiv:astro-ph/0409575.
- Mazzali, P.A., Iwamoto, K., Nomoto, K., 2000. A Spectroscopic Analysis of the Energetic Type Ic Hypernova SN 1997EF. *The Astrophysical Journal* 545, 407–419. doi:10.1086/317808, arXiv:astro-ph/0007222.
- Metzger, B.D., Margalit, B., Kasen, D., Quataert, E., 2015. The diversity of transients from magnetar birth in core collapse supernovae. *Monthly Notices of the Royal Astronomical Society* 454, 3311–3316. doi:10.1093/mnras/stv2224, arXiv:1508.02712.
- Milisavljevic, D., Margutti, R., Parrent, J.T., Soderberg, A.M., Fesen, R.A., Mazzali, P., Maeda, K., Sanders, N.E., Cenko, S.B., Silverman, J.M., Filippenko, A.V., Kamble, A., Chakraborti, S., Drout, M.R., Kirshner, R.P., Pickering, T.E., Kawabata, K., Hattori, T., Hsiao, E.Y., Stritzinger, M.D., Marion, G.H., Vinko, J., Wheeler, J.C., 2015. The Broad-lined Type Ic SN 2012ap and the Nature of Relativistic Supernovae Lacking a Gamma-Ray Burst Detection. *The Astrophysical Journal* 799, 51. doi:10.1088/0004-637X/799/1/51, arXiv:1408.1606.
- Milisavljevic, D., Patnaude, D.J., Chevalier, R.A., Raymond, J.C., Fesen, R.A., Margutti, R., Conner, B., Banovetz, J., 2018. Evidence for a Pulsar Wind Nebula in the Type Ib Peculiar Supernova SN 2012au. *The Astrophysical Journal Letters* 864, L36. doi:10.3847/2041-8213/aadd4e, arXiv:1809.01141.
- Modjaz, M., Gutiérrez, C.P., Arcavi, I., 2019. New regimes in the observation of core-collapse supernovae. *Nature Astronomy* 3, 717–724. doi:10.1038/s41550-019-0856-2, arXiv:1908.02476.
- Modjaz, M., Liu, Y.Q., Bianco, F.B., Graur, O., 2016. The Spectral SN-GRB Connection: Systematic Spectral Comparisons between Type Ic Supernovae and Broad-lined Type Ic Supernovae with and without Gamma-Ray Bursts. *The Astrophysical Journal* 832, 108. doi:10.3847/

0004-637X/832/2/108, arXiv:1509.07124.

- Moriya, T.J., 2024. Superluminous supernovae. arXiv e-prints , arXiv:2407.12302doi:10.48550/arXiv.2407.12302, arXiv:2407.12302.
- Moriya, T.J., Murase, K., Kashiyama, K., Blinnikov, S.I., 2022. Stripped-envelope supernova light-curve bumps caused by variable thermal energy injection from magnetar spin down. arXiv e-prints , arXiv:2202.03082arXiv:2202.03082.
- Müller, B., Tauris, T.M., Heger, A., Banerjee, P., Qian, Y.Z., Powell, J., Chan, C., Gay, D.W., Langer, N., 2019. Three-dimensional simulations of neutrino-driven core-collapse supernovae from low-mass single and binary star progenitors. Monthly Notices of the Royal Astronomical Society 484, 3307–3324. doi:10.1093/mnras/stz216, arXiv:1811.05483.
- Nicholl, M., 2021. Superluminous supernovae: an explosive decade. Astronomy and Geophysics 62, 5.34–5.42. doi:10.1093/astrogeo/atab092, arXiv:2109.08697.
- Nicholl, M., Guillochon, J., Berger, E., 2017. The Magnetar Model for Type I Superluminous Supernovae. I. Bayesian Analysis of the Full Multicolor Light-curve Sample with MOSFiT. The Astrophysical Journal 850, 55. doi:10.3847/1538-4357/aa9334, arXiv:1706.00825.
- Nicholl, M., Smartt, S.J., 2016. Seeing double: the frequency and detectability of double-peaked superluminous supernova light curves. Monthly Notices of the Royal Astronomical Society 457, L79–L83. doi:10.1093/mnrasl/slv210, arXiv:1511.03740.
- Nicholl, M., Smartt, S.J., Jerkstrand, A., Inserra, C., Sim, S.A., Chen, T.W., Benetti, S., Fraser, M., Gal-Yam, A., Kankare, E., Maguire, K., Smith, K., Sullivan, M., Valenti, S., Young, D.R., Baltay, C., Bauer, F.E., Baumont, S., Bersier, D., Botticella, M.T., Childress, M., Dennefeld, M., Della Valle, M., Elias-Rosa, N., Feindt, U., Galbany, L., Hadjyska, E., Le Guillou, L., Leloudas, G., Mazzali, P., McKinnon, R., Polshaw, J., Rabinowitz, D., Rostami, S., Scalzo, R., Schmidt, B.P., Schulze, S., Sollerman, J., Taddia, F., Yuan, F., 2015. On the diversity of superluminous supernovae: ejected mass as the dominant factor. Monthly Notices of the Royal Astronomical Society 452, 3869–3893. doi:10.1093/mnras/stv1522, arXiv:1503.03310.
- Nomoto, K., 1984. Evolution of 8-10 solar mass stars toward electron capture supernovae. I - Formation of electron-degenerate O + NE + MG cores. The Astrophysical Journal 277, 791–805. doi:10.1086/161749.
- Omand, C.M.B., Jerkstrand, A., 2023. Toward nebular spectral modeling of magnetar-powered supernovae. Astronomy & Astrophysics 673, A107. doi:10.1051/0004-6361/202245406, arXiv:2211.04502.
- Pandey, S.B., Kumar, A., Kumar, B., Anupama, G.C., Srivastav, S., Sahu, D.K., Vinko, J., Aryan, A., Pastorello, A., Benetti, S., Tomasella, L., Singh, A., Moskvitin, A.S., Sokolov, V.V., Gupta, R., Misra, K., Ochner, P., Valenti, S., 2021. Photometric, polarimetric, and spectroscopic studies of the luminous, slow-decaying Type Ib SN 2012au. Monthly Notices of the Royal Astronomical Society 507, 1229–1253. doi:10.1093/mnras/stab1889, arXiv:2106.15856.
- Papish, O., Soker, N., 2011. Exploding core collapse supernovae with jittering jets. Monthly Notices of the Royal Astronomical Society 416, 1697–1702. doi:10.1111/j.1365-2966.2011.18671.x, arXiv:1103.1554.
- Parrent, J., Branch, D., Troxel, M.A., Casebeer, D., Jeffery, D.J., Ketchum, W., Baron, E., Serduke, F.J.D., Filippenko, A.V., 2007. Direct Analysis of Spectra of the Unusual Type Ib Supernova 2005bf. Publications of the Astronomical Society of the Pacific 119, 135–142. doi:10.1086/512494, arXiv:astro-ph/0701198.
- Pastorello, A., Smartt, S.J., Mattila, S., Eldridge, J.J., Young, D., Itagaki, K., Yamaoka, H., Navasardyan, H., Valenti, S., Patat, F., Agnoletto, I., Augusteijn, T., Benetti, S., Cappellaro, E., Boles, T., Bonnet-Bidaud, J.M., Botticella, M.T., Bufano, F., Cao, C., Deng, J., Dennefeld, M., Elias-Rosa, N., Harutyunyan, A., Keenan, F.P., Iijima, T., Lorenzi, V., Mazzali, P.A., Meng, X., Nakano, S., Nielsen, T.B., Smoker, J.V., Stanishev, V., Turatto, M., Xu, D., Zampieri, L., 2007. A giant outburst two years before the core-collapse of a massive star. Nature 447, 829–832. doi:10.1038/nature05825, arXiv:astro-ph/0703663.
- Patat, F., Cappellaro, E., Danziger, J., Mazzali, P.A., Sollerman, J., Augusteijn, T., Brewer, J., Doublier, V., Gonzalez, J.F., Hainaut, O., Lidman, C., Leibundgut, B., Nomoto, K., Nakamura, T., Spyromilio, J., Rizzi, L., Turatto, M., Walsh, J., Galama, T.J., van Paradijs, J., Kouveliotou, C., Vreeswijk, P.M., Frontera, F., Masetti, N., Palazzi, E., Pian, E., 2001. The Metamorphosis of SN 1998bw. The Astrophysical Journal 555, 900–917. doi:10.1086/321526, arXiv:astro-ph/0103111.
- Pauldrach, A.W.A., Vanbeveren, D., Hoffmann, T.L., 2012. Radiation-driven winds of hot luminous stars XVI. Expanding atmospheres of massive and very massive stars and the evolution of dense stellar clusters. Astronomy & Astrophysics 538, A75. doi:10.1051/0004-6361/201117621, arXiv:1107.0654.
- Pearson, K., 1901. Liii. on lines and planes of closest fit to systems of points in space. The London, Edinburgh, and Dublin Philosophical Magazine and Journal of Science 2, 559–572. URL: <https://doi.org/10.1080/14786440109462720>, doi:10.1080/14786440109462720, arXiv:<https://doi.org/10.1080/14786440109462720>.
- Perley, D.A., Sollerman, J., Schulze, S., Yao, Y., Fremling, C., Gal-Yam, A., Ho, A.Y.Q., Yang, Y., Kool, E.C., Irani, I., Yan, L., Andreoni, I., Baade, D., Bellm, E.C., Brink, T.G., Chen, T.W., Cikota, A., Coughlin, M.W., Dahiwale, A., Dekany, R., Duev, D.A., Filippenko, A.V., Hoeflich, P., Kasliwal, M.M., Kulkarni, S.R., Lunnan, R., Masci, F.J., Maund, J.R., Medford, M.S., Riddle, R., Rosnet, P., Shupe, D.L., Strotjohann, N.L., Tzanidakis, A., Zheng, W., 2022. The Type Icn SN 2021csp: Implications for the Origins of the Fastest Supernovae and the Fates of Wolf-Rayet Stars. The Astrophysical Journal 927, 180. doi:10.3847/1538-4357/ac478e, arXiv:2111.12110.
- Pignata, G., Stritzinger, M., Soderberg, A., Mazzali, P., Phillips, M.M., Morrell, N., Anderson, J.P., Boldt, L., Campillay, A., Contreras, C., Folatelli, G., Förster, F., González, S., Hamuy, M., Krzeminski, W., Maza, J., Roth, M., Salgado, F., Levesque, E.M., Rest, A., Crain, J.A., Foster, A.C., Haislip, J.B., Ivarsen, K.M., LaCluyze, A.P., Nysewander, M.C., Reichart, D.E., 2011. SN 2009bb: A Peculiar Broad-lined Type Ic Supernova. The Astrophysical Journal 728, 14. doi:10.1088/0004-637X/728/1/14, arXiv:1011.6126.
- Podsiadlowski, P., Langer, N., Poelarends, A.J.T., Rappaport, S., Heger, A., Pfahl, E., 2004. The Effects of Binary Evolution on the Dynamics of Core Collapse and Neutron Star Kicks. The Astrophysical Journal 612, 1044–1051. doi:10.1086/421713, arXiv:astro-ph/0309588.
- Prentice, S.J., Mazzali, P.A., 2017. A physically motivated classification of stripped-envelope supernovae. Monthly Notices of the Royal Astronomical Society 469, 2672–2694. doi:10.1093/mnras/stx980, arXiv:1704.06635.
- Prentice, S.J., Mazzali, P.A., Pian, E., Gal-Yam, A., Kulkarni, S.R., Rubin, A., Corsi, A., Fremling, C., Sollerman, J., Yaron, O., Arcavi, I., Zheng, W., Kasliwal, M.M., Filippenko, A.V., Cenko, S.B., Cao, Y., Nugent, P.E., 2016. The bolometric light curves and physical parameters of stripped-envelope supernovae. Monthly Notices of the Royal Astronomical Society 458, 2973–3002. doi:10.1093/mnras/stw299,

[arXiv:1602.01736](https://arxiv.org/abs/1602.01736).

- Puls, J., Vink, J.S., Najarro, F., 2008. Mass loss from hot massive stars. *Astronomy and Astrophysics Reviews* 16, 209–325. doi:10.1007/s00159-008-0015-8, [arXiv:0811.0487](https://arxiv.org/abs/0811.0487).
- Quimby, R.M., Kulkarni, S.R., Kasliwal, M.M., Gal-Yam, A., Arcavi, I., Sullivan, M., Nugent, P., Thomas, R., Howell, D.A., Nakar, E., Bildsten, L., Theissen, C., Law, N.M., Dekany, R., Rahmer, G., Hale, D., Smith, R., Ofek, E.O., Zolkower, J., Velur, V., Walters, R., Henning, J., Bui, K., McKenna, D., Poznanski, D., Cenko, S.B., Levitan, D., 2011. Hydrogen-poor superluminous stellar explosions. *Nature* 474, 487–489. doi:10.1038/nature10095, [arXiv:0910.0059](https://arxiv.org/abs/0910.0059).
- Rasmussen, C.E., Williams, C.K.I., 2005. Gaussian Processes for Machine Learning. The MIT Press. URL: <https://doi.org/10.7551/mitpress/3206.001.0001>, doi:10.7551/mitpress/3206.001.0001.
- Rodríguez, Ó., Nakar, E., Maoz, D., 2024. Stripped-envelope supernova light curves argue for central engine activity. *Nature* 628, 733–735. doi:10.1038/s41586-024-07262-x, [arXiv:2404.10846](https://arxiv.org/abs/2404.10846).
- Sahu, D.K., Tanaka, M., Anupama, G.C., Gurugubelli, U.K., Nomoto, K., 2009. The Broad-Line Type Ic Supernova SN 2007ru: Adding to the Diversity of Type Ic Supernovae. *The Astrophysical Journal* 697, 676–683. doi:10.1088/0004-637X/697/1/676, [arXiv:0805.3201](https://arxiv.org/abs/0805.3201).
- Shishkin, D., Soker, N., 2023. The implications of large binding energies of massive stripped core collapse supernova progenitors on the explosion mechanism. *Monthly Notices of the Royal Astronomical Society* 522, 438–445. doi:10.1093/mnras/stad889, [arXiv:2301.05144](https://arxiv.org/abs/2301.05144).
- Siebert, M.R., DeCoursey, C., Coulter, D.A., Engesser, M., Pierel, J.D.R., Rest, A., Egami, E., Shahbandeh, M., Chen, W., Fox, O.D., Zenati, Y., Moriya, T.J., Bunker, A.J., Cargile, P.A., Curti, M., Eisenstein, D.J., Gezari, S., Gomez, S., Guolo, M., Johnson, B.D., Joshi, B.A., Karmen, M., Maiolino, R., Quimby, R.M., Robertson, B., Strolger, L.G., Sun, F., Wang, Q., Wevers, T., 2024. Discovery of a Relativistic Stripped-envelope Type Ic-BL Supernova at  $z = 2.83$  with JWST. *The Astrophysical Journal Letters* 972, L13. doi:10.3847/2041-8213/ad6c32, [arXiv:2406.05076](https://arxiv.org/abs/2406.05076).
- Smartt, S.J., 2009. Progenitors of Core-Collapse Supernovae. *Annual Review of Astron and Astrophys* 47, 63–106. doi:10.1146/annurev-astro-082708-101737, [arXiv:0908.0700](https://arxiv.org/abs/0908.0700).
- Smith, N., 2014. Mass Loss: Its Effect on the Evolution and Fate of High-Mass Stars. *Annual Review of Astron and Astrophys* 52, 487–528. doi:10.1146/annurev-astro-081913-040025, [arXiv:1402.1237](https://arxiv.org/abs/1402.1237).
- Smith, N., Gehrz, R.D., Campbell, R., Kassis, M., Le Mignant, D., Kuluhiva, K., Filippenko, A.V., 2011. Episodic mass loss in binary evolution to the Wolf-Rayet phase: Keck and HST proper motions of RY Scuti's nebula. *Monthly Notices of the Royal Astronomical Society* 418, 1959–1972. doi:10.1111/j.1365-2966.2011.19614.x, [arXiv:1105.2329](https://arxiv.org/abs/1105.2329).
- Smith, N., Owocki, S.P., 2006. On the Role of Continuum-driven Eruptions in the Evolution of Very Massive Stars and Population III Stars. *The Astrophysical Journal Letters* 645, L45–L48. doi:10.1086/506523, [arXiv:astro-ph/0606174](https://arxiv.org/abs/astro-ph/0606174).
- Soker, N., 2010. Applying the jet feedback mechanism to core-collapse supernova explosions. *Monthly Notices of the Royal Astronomical Society* 401, 2793–2798. doi:10.1111/j.1365-2966.2009.15862.x, [arXiv:0909.5276](https://arxiv.org/abs/0909.5276).
- Soker, N., 2022a. Boosting Jittering Jets by Neutrino Heating in Core Collapse Supernovae. *Research in Astronomy and Astrophysics* 22, 095007. doi:10.1088/1674-4527/ac7cbc, [arXiv:2202.05556](https://arxiv.org/abs/2202.05556).
- Soker, N., 2022b. Imprints of the Jittering Jets Explosion Mechanism in the Morphology of the Supernova Remnant SNR 0540-69.3. *Research in Astronomy and Astrophysics* 22, 035019. doi:10.1088/1674-4527/ac49e6, [arXiv:2109.10230](https://arxiv.org/abs/2109.10230).
- Soker, N., 2022c. Powering Luminous Core Collapse Supernovae with Jets. *The Astrophysical Journal* 935, 108. doi:10.3847/1538-4357/ac822d, [arXiv:2205.09560](https://arxiv.org/abs/2205.09560).
- Soker, N., 2022d. The Role of Jets in Exploding Supernovae and in Shaping their Remnants. *Research in Astronomy and Astrophysics* 22, 122003. doi:10.1088/1674-4527/ac9782, [arXiv:2208.04875](https://arxiv.org/abs/2208.04875).
- Soker, N., 2023. Implications of post-kick jets in core-collapse supernovae. *Monthly Notices of the Royal Astronomical Society* 520, 4404–4409. doi:10.1093/mnras/stad379, [arXiv:2210.13792](https://arxiv.org/abs/2210.13792).
- Soker, N., 2024. Supernovae in 2023 (review): possible breakthroughs by late observations. *The Open Journal of Astrophysics* 7, 31. doi:10.33232/001c.117147, [arXiv:2311.17732](https://arxiv.org/abs/2311.17732).
- Soker, N., Gilkis, A., 2017. Magnetar-powered Superluminous Supernovae Must First Be Exploded by Jets. *The Astrophysical Journal* 851, 95. doi:10.3847/1538-4357/aa9c83, [arXiv:1708.08356](https://arxiv.org/abs/1708.08356).
- Solar, M., Michałowski, M.J., Nadolny, J., Galbany, L., Hjorth, J., Zapartas, E., Sollerman, J., Hunt, L., Klose, S., Koprowski, M., Leśniewska, A., Małkowski, M., Nicuesa Guelbenzu, A.M., Ryzhov, O., Savaglio, S., Schady, P., Schulze, S., de Ugarte Postigo, A., Vergani, S.D., Watson, D., Wróblewski, R., 2024. Binary progenitor systems for Type Ic supernovae. *Nature Communications* 15, 7667. doi:10.1038/s41467-024-51863-z, [arXiv:2409.01906](https://arxiv.org/abs/2409.01906).
- Sollerman, J., Fransson, C., Barbarino, C., Fremling, C., Horesh, A., Kool, E., Schulze, S., Sfaradi, I., Yang, S., Bellm, E.C., Burruss, R., Cunningham, V., De, K., Drake, A.J., Golkhou, V.Z., Green, D.A., Kasliwal, M., Kulkarni, S., Kupfer, T., Laher, R.R., Masci, F.J., Rodriguez, H., Rusholme, B., Williams, D.R.A., Yan, L., Zolkower, J., 2020. Two stripped envelope supernovae with circumstellar interaction. But only one really shows it. *Astronomy & Astrophysics* 643, A79. doi:10.1051/0004-6361/202038960, [arXiv:2009.04154](https://arxiv.org/abs/2009.04154).
- Sukhbold, T., Ertl, T., Woosley, S.E., Brown, J.M., Janka, H.T., 2016. Core-collapse Supernovae from 9 to 120 Solar Masses Based on Neutrino-powered Explosions. *The Astrophysical Journal* 821, 38. doi:10.3847/0004-637X/821/1/38, [arXiv:1510.04643](https://arxiv.org/abs/1510.04643).
- Taddia, F., Sollerman, J., Fremling, C., Barbarino, C., Karamehmetoglu, E., Arcavi, I., Cenko, S.B., Filippenko, A.V., Gal-Yam, A., Hirayama, D., Hosseinzadeh, G., Howell, D.A., Kulkarni, S.R., Laher, R., Lunnan, R., Masci, F., Nugent, P.E., Nyholm, A., Perley, D.A., Quimby, R., Silverman, J.M., 2019. Analysis of broad-lined Type Ic supernovae from the (intermediate) Palomar Transient Factory. *Astronomy & Astrophysics* 621, A71. doi:10.1051/0004-6361/201834429, [arXiv:1811.09544](https://arxiv.org/abs/1811.09544).
- Taddia, F., Sollerman, J., Fremling, C., Karamehmetoglu, E., Quimby, R.M., Gal-Yam, A., Yaron, O., Kasliwal, M.M., Kulkarni, S.R., Nugent, P.E., Smadja, G., Tao, C., 2018. PTF11mb: First analog of supernova 2005bf. Long-rising, double-peaked supernova Ic from a massive progenitor. *Astronomy & Astrophysics* 609, A106. doi:10.1051/0004-6361/201629874, [arXiv:1709.08386](https://arxiv.org/abs/1709.08386).

## Magnetar-driven Light Curves of SESNe

- Taddia, F., Sollerman, J., Leloudas, G., Stritzinger, M.D., Valenti, S., Galbany, L., Kessler, R., Schneider, D.P., Wheeler, J.C., 2015. Early-time light curves of Type Ib/c supernovae from the SDSS-II Supernova Survey. *Astronomy & Astrophysics* 574, A60. doi:10.1051/0004-6361/201423915, arXiv:1408.4084.
- Tominaga, N., Tanaka, M., Nomoto, K., Mazzali, P.A., Deng, J., Maeda, K., Umeda, H., Modjaz, M., Hicken, M., Challis, P., Kirshner, R.P., Wood-Vasey, W.M., Blake, C.H., Bloom, J.S., Skrutskie, M.F., Szentgyorgyi, A., Falco, E.E., Inada, N., Minezaki, T., Yoshii, Y., Kawabata, K., Iye, M., Anupama, G.C., Sahu, D.K., Prabhu, T.P., 2005. The Unique Type Ib Supernova 2005bf: A WN Star Explosion Model for Peculiar Light Curves and Spectra. *The Astrophysical Journal Letters* 633, L97–L100. doi:10.1086/498570, arXiv:astro-ph/0509557.
- Utrobin, V.P., Wongwathanarat, A., Janka, H.T., Müller, E., 2015. Supernova 1987A: neutrino-driven explosions in three dimensions and light curves. *Astronomy & Astrophysics* 581, A40. doi:10.1051/0004-6361/201425513, arXiv:1412.4122.
- Wang, L., Wheeler, J.C., 1998. The Supernova-Gamma-Ray Burst Connection. *The Astrophysical Journal Letters* 504, L87–L90. doi:10.1086/311580, arXiv:astro-ph/9806212.
- Wang, L.J., Han, Y.H., Xu, D., Wang, S.Q., Dai, Z.G., Wu, X.F., Wei, J.Y., 2016. Solving the  $^{56}\text{Ni}$  Puzzle of Magnetar-powered Broad-lined Type IC Supernovae. *The Astrophysical Journal* 831, 41. doi:10.3847/0004-637X/831/1/41, arXiv:1608.05482.
- Wang, L.J., Yu, H., Liu, L.D., Wang, S.Q., Han, Y.H., Xu, D., Dai, Z.G., Qiu, Y.L., Wei, J.Y., 2017a. Evidence for Magnetar Formation in Broad-lined Type Ic Supernovae 1998bw and 2002ap. *The Astrophysical Journal* 837, 128. doi:10.3847/1538-4357/aa5ff5, arXiv:1610.09061.
- Wang, S.Q., Cano, Z., Wang, L.J., Zheng, W., Dai, Z.G., Filippenko, A.V., Liu, L.D., 2017b. Modeling The Most Luminous Supernova Associated with a Gamma-Ray Burst, SN 2011kl. *The Astrophysical Journal* 850, 148. doi:10.3847/1538-4357/aa95c5, arXiv:1707.08515.
- Wheeler, J.C., Chatzopoulos, E., Vinkó, J., Tuminello, R., 2017. Circumstellar Interaction Models for the Bolometric Light Curve of Type I Superluminous SN 2017egm. *The Astrophysical Journal Letters* 851, L14. doi:10.3847/2041-8213/aa9d84, arXiv:1710.04994.
- Wheeler, J.C., Johnson, V., Clocchiatti, A., 2015. Analysis of late-time light curves of Type IIb, Ib and Ic supernovae. *Monthly Notices of the Royal Astronomical Society* 450, 1295–1307. doi:10.1093/mnras/stv650, arXiv:1411.5975.
- Woosley, S.E., 2010. Bright Supernovae from Magnetar Birth. *The Astrophysical Journal Letters* 719, L204–L207. doi:10.1088/2041-8205/719/2/L204, arXiv:0911.0698.
- Woosley, S.E., Bloom, J.S., 2006. The Supernova Gamma-Ray Burst Connection. *Annual Review of Astron and Astrophys* 44, 507–556. doi:10.1146/annurev.astro.43.072103.150558, arXiv:astro-ph/0609142.
- Woosley, S.E., Eastman, R.G., Weaver, T.A., Pinto, P.A., 1994. SN 1993J: A Type IIb Supernova. *The Astrophysical Journal* 429, 300. doi:10.1086/174319.
- Woosley, S.E., Langer, N., Weaver, T.A., 1995. The Presupernova Evolution and Explosion of Helium Stars That Experience Mass Loss. *The Astrophysical Journal* 448, 315. doi:10.1086/175963.
- Yamada, S., Nagakura, H., Akaho, R., Harada, A., Furusawa, S., Iwakami, W., Okawa, H., Matsufuru, H., Sumiyoshi, K., 2024. Physical mechanism of core-collapse supernovae that neutrinos drive. *Proceedings of the Japan Academy, Series B* 100, 190–233. doi:10.2183/pjab.100.015.
- Yoon, S.C., 2015. Evolutionary Models for Type Ib/c Supernova Progenitors. *PASA* 32, e015. doi:10.1017/pasa.2015.16, arXiv:1504.01205.
- Yoon, S.C., Woosley, S.E., Langer, N., 2010. Type Ib/c Supernovae in Binary Systems. I. Evolution and Properties of the Progenitor Stars. *The Astrophysical Journal* 725, 940–954. doi:10.1088/0004-637X/725/1/940, arXiv:1004.0843.
- Yu, Y.W., Zhu, J.P., Li, S.Z., Lü, H.J., Zou, Y.C., 2017. A Statistical Study of Superluminous Supernovae Using the Magnetar Engine Model and Implications for Their Connection with Gamma-Ray Bursts and Hypernovae. *The Astrophysical Journal* 840, 12. doi:10.3847/1538-4357/aa6c27, arXiv:1704.01682.
- Zhu, J.P., Liu, L.D., Yu, Y.W., Mandel, I., Hirai, R., Zhang, B., Chen, A., 2024. Bumpy Superluminous Supernovae Powered by a Magnetar–Star Binary Engine. *The Astrophysical Journal Letters* 970, L42. doi:10.3847/2041-8213/ad63a8, arXiv:2405.01224.